sample) was almost $70 for the PCR-SSCP analysis, followed by 16S rDNA sequencing. The cost of the PCR-SSCP method can be reduced because the high reproducibility of PCR-SSCP enables the grouping of strains between different samples.

In this study, we evaluated the PCR-SSCP process as a grouping method for isolated strains from plate count analysis and showed good correlation between the PCR-SSCP analysis and 16S rDNA sequencing. Among 180 strains from various foods, 2.2% were misgrouped due to their phylogenetic relationships. This is not a substantial problem of the PCR-SSCP method because the most important aspect of this grouping method for isolates used by food suppliers is the practical usefulness. The PCR-SSCP method meets these requirements in various aspects, such as sufficient accuracy, high throughput, high reproducibility, and ease of operation. This PCR-SSCP method can also be used as the grouping method of isolates followed by identification using the identification kits and classical identification by biochemical characterization.

ACKNOWLEDGMENTS

This work was partially supported by the National Food Research Institute of Japan (project: Development of evaluation and management methods for supply of safe, reliable and functional food and farm products) and Japanese Ministry of Health, Labour and Welfare (H19-011)

REFERENCES

1. Blackwood, K. S., C. Y. Turenne, D. Harmsen, and A. M. Kabani. 2004. Reassessment of sequence-based targets for identification of *Bacillus* species. *J. Clin. Microbiol.* 42:1626–1630.
2. Brosius, J., M. L. Palmer, P. J. Kennedy, and H. F. Noller. 1978. Complete nucleotide sequence of a 16S ribosomal RNA gene from *Escherichia coli*. *Proc. Natl. Acad. Sci. USA* 75:4801–4805.
3. Chakravorty, S., D. Helb, M. Burday, N. Connell, and D. Alland. 2007. A detailed analysis of 16S ribosomal RNA gene segments for the diagnosis of pathogenic bacteria. *J. Microbiol. Methods* 69:330–339.
4. Clayton, R. A., G. Sutton, P. S. Hinkle, Jr., C. Bult, and C. Fields. 1995. Intraspecific variation in small-subunit rRNA sequences in GenBank: why single sequences may not adequately represent prokaryotic taxa. *Int. J. Syst. Bacteriol.* 45:595–599.
5. Collins, M. D., P. A. Lawson, A. Willems, J. J. Cordoba, J. Fernandez-Garayzabal, P. Garcia, J. Cai, H. Hippe, and J. A. Farrow. 1994. The phylogeny of the genus *Clostridium*: proposal of five new genera and eleven new species combinations. *Int. J. Syst. Bacteriol.* 44: 812–826.
6. De Angelis, M., R. Di Cagno, G. Gallo, S. Curci, C. Siragusa, C. Crecchio, E. Parente, and M. Gobbetti. 2007. Molecular and functional characterization of *Lactobacillus sanfranciscensis*. *Int. J. Food Microbiol.* 28:69–82.
7. Don, R. H., P. T. Cox, B. J. Wainwright, K. Baker, and J. S. Mattick. 1991. "Touchdown" PCR to circumvent spurious priming during gene amplification. *Nucleic Acids Res.* 19:4008.
8. Drancourt, M., C. Bollet, A. Carta, and P. Rousselier. 2001. Phylogenetic analyses of *Klebsiella* species delineate *Klebsiella* and *Raoultella* gen. nov., with description of *Raoultella ornithinolytica* comb. nov., *Raoultella terrigena* comb. nov. and *Raoultella planticola* comb. nov. *Int. J. Syst. Evol. Microbiol.* 51:925–932.
9. Duthoit, F., J. J. Godon, and M. C. Montel. 2003. Bacterial community dynamics during production of registered designation of origin Salers cheese as evaluated by 16S rRNA gene single-strand conformation polymorphism analysis. *Appl. Environ. Microbiol.* 69: 3840–3848.
10. Ercolini, D. 2004. PCR-DGGE fingerprinting: novel strategies for detection of microbes in food. *J. Microbiol. Methods* 59:217–234.
11. Fogel, G. B., C. R. Collins, J. Li, and C. F. Brunk. 1999. Prokaryotic genome size and SSU rDNA copy number: estimation of microbial relative abundance from a mixed population. *Microb. Ecol.* 38:93–113.
12. Grahn, N., M. Hmani-Aifa, K. Fransen, P. Soderkvist, and H. J. Monstein. 2005. Molecular identification of Helicobacter DNA present in human colorectal adenocarcinomas by 16S rDNA PCR amplification and pyrosequencing analysis. *J. Med. Microbiol.* 54:1031–1035.
13. Hill, K. E., C. E. Davies, M. J. Wilson, P. Stephens, M. A. O. Lewis, V. Hall, J. Brazier, and D. W. Thomas. 2002. Heterogeneity within the gram-positive anaerobic cocci demonstrated by analysis of 16S–23S intergenic ribosomal RNA polymorphisms. *J. Med. Microbiol.* 51:949–957.
14. Hill, W. E., A. Dahlberg, R. A. Garrett, P. B. Moore, D. Schlessinger, and J. R. Warner (ed.). 1990. The ribosome: structure, function and evolution. American Society for Microbiology, Washington, D.C.
15. Lee, D. H., Y. G. Zo, and S. J. Kim. 1996. Nonradioactive method to study genetic profiles of natural bacterial communities by PCR-single-strand-conformation polymorphism. *Appl. Environ. Microbiol.* 62:3112–3120.
16. Muyzer, G., E. C. De Waal, and A. G. Uitterlinden. 1993. Profiling of complex microbial populations by denaturing gradient gel electrophoresis analysis of polymerase chain reaction-amplified genes coding for 16S rRNA. *Appl. Environ. Microbiol.* 59:695–700.
17. Mylvaganam, S., and P. P. Dennis. 1992. Sequence heterogeneity between the two genes encoding 16S rRNA from the halophilic archaebacterium *Haloarcula marismortui*. *Genetics* 130:399–410.
18. Neefs, J. M., Y. Van de Peer, L. Hendriks, and R. D. Wachter. 1990. Compilation of small ribosomal subunit RNA sequences. *Nucleic Acids Res.* 18:2237–2317.
19. Orita, M., H. Iwahana, H. Kanazawa, K. Hayashi, and T. Sekiya. 1989. Detection of polymorphisms of human DNA by gel electrophoresis as single-strand conformation polymorphisms. *Proc. Natl. Acad. Sci. USA* 86:2766–2770.
20. Peters, S., S. Koschinsky, F. Schwieger, and C. C. Tebbe. 2000. Succession of microbial communities during hot composting as detected by PCR-single-strand-conformation polymorphism-based genetic profiles of small-subunit rRNA genes. *Appl. Environ. Microbiol.* 66: 930–936.
21. Rantsiou, K., R. Urso, L. Iacumin, C. Cantoni, P. Cattaneo, G. Comi, and L. Cocolin, L. 2005. Culture-dependent and independent methods to investigate the microbial ecology of Italian fermented sausages. *Appl. Environ. Microbiol.* 71:1977–1986.
22. Schwieger, F., and C. C. Tebbe. 1998. A new approach to utilize PCR-single-strand-conformation polymorphism for 16S rRNA gene-based microbial community analysis. *Appl. Environ. Microbiol.* 64: 4870–4876.
23. Takahashi, H., B. Kimura, M. Yoshikawa, S. Gotou, I. Watanabe, and T. Fujii. 2004. Direct detection and identification of lactic acid bacteria in a food processing plant and in meat products using denaturing gradient gel electrophoresis. *J. Food Prot.* 67:2515–2520.
24. Takahashi, T., I. Satoh, and N. Kikuchi. 1999. Phylogenetic relationships of 38 taxa of the genus *Staphylococcus* based on 16S rRNA gene sequence analysis. *Int. J. Syst. Bacteriol.* 49:725–728.
25. Turenne, C. Y., E. Witwicki, D. J. Hoban, J. A. Karlowsky, and A. M. Kabani. 2000. Rapid identification of bacteria from positive blood cultures by fluorescence-based PCR-single-strand conformation polymorphism analysis of the 16S rRNA gene. *J. Clin. Microbiol.* 38:513–520.
26. Vandamme, P., J. F. Bernardet, P. Segers, K. Kersters, and B. Holmes. 1994. New perspectives in the classification of the *Flavobacteria*: description of *Chryseobacterium* gen. nov., *Bergeyella* gen. nov., and *Empedobacter* nom. rev. *Int. J. Syst. Bacteriol.* 44:827–831.
27. Weisburg, W. G., S. M. Barns, D. A. Pelletier, and D. J. Lane. 1991. 16S ribosomal DNA amplification for phylogenetic study. *J. Bacteriol.* 173:697–703.
28. Widjojoatmodjo, M. N., A. C. Fluit, and J. Verhoef. 1994. Rapid identification of bacteria by PCR-single-strand conformation polymorphism. *J. Clin. Microbiol.* 32:3002–3007.
29. Yu, Z., and M. Morrison. 2004. Comparisons of different hypervariable regions of *rrs* genes for use in fingerprinting of microbial communities by PCR-denaturing gradient gel electrophoresis. *Appl. Environ. Microbiol.* 70:4800–4806.

Available online at www.sciencedirect.com
ScienceDirect
Journal of Microbiological Methods 72 (2008) 313–320
Journal of Microbiological Methods
www.elsevier.com/locate/jmicmeth

Multiple-locus variable-number of tandem-repeats analysis distinguishes *Vibrio parahaemolyticus* pandemic O3:K6 strains

Bon Kimura [a,*], Yohko Sekine [a], Hajime Takahashi [a], Yuichiro Tanaka [a], Hiromi Obata [b], Akemi Kai [b], Satoshi Morozumi [b], Tateo Fujii [a]

[a] *Tokyo University of Marine Science and Technology, Department of Food Science and Technology, Minato Tokyo 108-8477, Japan*
[b] *Tokyo Metropolitan Institute of Public Health, Department of Microbiology, Shinjuku Tokyo 169-0073, Japan*

Received 6 November 2007; received in revised form 15 December 2007; accepted 31 December 2007
Available online 10 January 2008

Abstract

A specific serotype of *Vibrio parahaemolyticus*, O3:K6, has recently been linked to epidemics of gastroenteritis in Southeast Asia, Japan, and North America. These pandemic O3:K6 strains appear to have recently spread across continents from a single origin to reach global coverage, based on profiling of strains by several molecular typing methods. In this study, variable-number tandem repeats (VNTR)-based fingerprinting was applied to clinical and environmental *V. parahaemolyticus* O3:K6 strains in an attempt to develop a molecular method with increased sensitivity for discriminating strains; the relative discriminatory powers were compared with ribotyping and pulsed-field gel electrophoresis (PFGE). All clinical strains tested were independent human isolates obtained from different outbreaks or from sporadic cases in Tokyo during the period from 1996 to 2003. Multiple-locus VNTR analysis (MLVA) was shown to have high resolution and reproducibility for typing of *V. parahaemolyticus* clones. MLVA analysis of 28 pandemic *V. parahaemolyticus* O3:K6 strains isolated from human cases produced 28 distinct VNTR patterns. The VNTR loci displayed between 2 and 15 alleles at each of eight loci with Nei's diversity index ranging from 0.35 and 0.91. These data demonstrated that MLVA is useful for individual strain typing of new O3:K6 strains, which appear to be closely related by other molecular methods.

Keywords: DNA typing; MLVA; *Vibrio parahaemolyticus*; VNTR

1. Introduction

Vibrio parahaemolyticus is a gram-negative marine bacterium that causes seafood-borne gastroenteritis; but not all strains have the same pathogenic potential. Infections are usually caused by *V. parahaemolyticus* of diverse serotypes, and until 1996, infections were characterized by sporadic cases caused by multiple, diverse serotypes. However, recent studies have shown the emergence of serotype O3:K6, a unique serotype that is characterized by the potential to spread and to be associated with infections more often than other serotypes. In February 1996, strains belonging to the O3:K6 serotype were first documented in Calcutta, India, and accounted for 50 to 80% of the strains of *V. parahaemolyticus* responsible for infections occurring annually since then (Okuda et al., 1997). Furthermore, strains belonging to the new O3:K6 serotype have been isolated from other Southeast Asian countries, from travelers at a quarantine station in Japan (Okuda et al., 1997), and from a food-borne outbreak in the United States (Centers for Disease Control and Prevention, 1999). These isolates possessed the *tdh* gene encoding thermostable direct hemolysin (TDH), lacked the *trh* gene encoding TDH-related hemolysin, and showed very similar profiles by several molecular methods (Matsumoto et al., 2000; Nasu et al., 2000; Wong et al., 2000), suggesting the presence of a common ancestor.

* Corresponding author. Mailing address: Department of Food Science and Technology, Faculty of Marine Science, Tokyo University of Marine Science and Technology, 4-5-7 Konan, Minato, Tokyo 108-8477, Japan. Tel./fax: +81 3 5463 0603.
E-mail address: kimubo@kaiyodai.ac.jp (B. Kimura).

0167-7012/$ - see front matter © 2008 Elsevier B.V. All rights reserved.
doi:10.1016/j.mimet.2007.12.014

A variety of molecular typing methods have been applied to *V. parahaemolyticus*; ribotyping (Bag et al., 1999; DePaola et al., 2003; Gendel et al., 2001), pulsed-field gel electrophoresis (PFGE) (Bag et al., 1999; Marshall et al., 1999), group-specific PCR (GS-PCR) (Matsumoto et al., 2000), arbitrarily primed PCR (AP-PCR) (Hara-Kudo et al., 2003; Matsumoto et al., 2000; Okuda et al., 1997), and multilocus sequence typing (MLST) (Chowdhury et al., 2004). However, newly identified O3:K6 strains are shown to be genetically homogeneous, and it makes difficult to distinguish them by above methods. Therefore, we decided to develop a method that targets the short tandem repeat sequences (TRs), which undergo rapid evolution in the bacterial genome. Increasingly, variable-number tandem repeats (VNTRs) have been used to discriminate among individual strains within several food- or waterborne pathogen with little genetic variation, including *Escherichia coli* O157:H7 (Lindstedt et al., 2004a; Noller et al., 2003), *Pseudomonas aeruginosa* (Onteniente et al., 2003), *Staphylococcus aureus* (Sabat et al., 2003), *Salmonella. enterica* subsp. *enterica* serovar Typhimurium (Lindstedt et al., 2004b). Short sequence repeats, including VNTRs, consist of unique DNA elements that are repeated in tandem. Individual strains within a bacterial species often maintain the same sequence elements but with different copy numbers, variation introduced by slipped-strand mispairing during DNA replication (Metzgar et al., 2001). Since sequence homologies between strains exist in the flanking-sequences, specific primers can be used to determine the variation in copy numbers of repeat units, reflecting intraspecific genetic diversity.

The primary aim of this study was to develop a high-resolution typing system for *V. parahaemolyticus* serotype O3:K6 based on polymorphisms at genomic VNTR loci. We demonstrate the utility of this approach by comparing PFGE results for clinical strains of *V. parahaemolyticus* serotype O3:K6 from different outbreaks in Tokyo occurring from 1996 to 2003. This study shows for the first time that clonal pandemic O3:K6 strains are distinguishable by differing VNTR patterns.

2. Materials and methods

2.1. Bacterial strains

All *V. parahaemolyticus* strains ($n=34$) were collected by the Tokyo Metropolitan Institute of Public Health and provided to the Food Microbiology Laboratory at the Tokyo University of Marine Science and Technology (Table 1). Among them, 28 were clinical strains isolated from single patients associated with different outbreaks or sporadic cases in Tokyo during the period from 1996 to 2003 and the other 6 strains were environmental strains isolated from either food or seawater during the period from 1999 to 2003. All *V. parahaemolyticus* strains were grown in LB broth or on LB agar (1.5% agar) with 3% sodium chloride. All strains were serotyped by the slide agglutination test with O- and K- antigen using commercially available antisera (*V. parahaemolyticus* antisera Seiken set, Denka Seiken, Tokyo, Japan), and the presence of the *tdh* gene and *trh* gene in the isolates were determined by the primers described previously (Okura et al., 2003).

2.2. GS-PCR

GS-PCR for *toxRS* sequence of the newly emerging *V. parahaemolyticus* serotype O3:K6 clones (*toxRS/new*) and old O3:K6 strains (*toxRS/old*) was performed according to the reports by Okura et al. (2003), and ORF8 PCR for detection of the f237 filamentous phage which is unique to the newly emerged O3:K6 clones (Nasu et al., 2000) was also performed (Okura et al., 2003).

2.3. Automated ribotyping

Ribotyping was carried out using the Qualicon RiboPrinter Microbial Characterization System (Qualicon, Inc., Wilmington, Del.) according to the manufacturer's instructions. Riboprint patterns for each strain were compared to the patterns produced for all other strains using the same restriction enzyme using the software supplied with the Riboprinter system. Strain-to-strain comparisons were used to define ribogroups, each consisting of patterns that were >0.90 similar. The sample number of the first pattern in each group became the label used to identify that group. The analysis software derived a single average pattern for each ribogroup, as well as information on the similarity of each pattern within the group to the group average pattern.

2.4. Typing O3:K6 strains by PFGE

PFGE typing of strains was performed on genomic DNA digested with restriction enzyme *Not* I, as described elsewhere (Hara-Kudo et al., 2003; Yeung et al., 2002) with minor modifications. All strains were grown overnight at 30 °C in LB broth. Bacteria were harvested by centrifugation and resuspended in 100 μl resuspension buffer (Bio-Rad Laboratories Ltd., Richmond, Calif.). Agarose plugs were prepared by mixing equal volumes of bacterial suspensions. Suspensions were transferred to disposable plug molds and cooled to 4 °C. Bacterial cells in the agarose plugs were treated with lysozyme solution at 25 °C for 2 h, after which, the plugs were suspended in 300 μl of proteinase buffer containing 3 μl of proteinase K and incubated at 50 °C for overnight. Agarose plugs were washed once with wash buffer, once with 1 mM PMSF, twice with wash buffer, and once with 0.1 × wash buffer with wash time of 1 h each. Agarose plugs containing genomic DNA were digested with 10 U of *Not* I (Takara Bio Inc., Shiga, Japan) at 25 °C overnight. PFGE was performed with 1% agarose gel (Seakem Agarose Gold; FMC Bioproducts, Rockland, Me.) on a CHEF-DR II apparatus (Bio-Rad) in 0.5 × TBE buffer at 14 °C. Electrophoresis was performed at 6 V/cm for 18 h with a 2- to 40- s linear ramp time.

2.5. Searching potential VNTRs

All VNTR loci were selected using MICAS (http://www.cdfd.org.in/micas/) (Sreenu et al., 2003) and the Tandem Repeat Finder program (http://tandem.biomath.mssm.edu/trf/trf.html) (Benson, 1999) from the entire genomic sequence of *V. parahaemolyticus* RIMD2210633, Kanagawa-phenomenon positive, serotype O3:K6 (Makino et al., 2003), GenBank

Table 1
Vibrio parahaemolyticus strains used in this study

Source	Strains[a]	Serotype[b]	Year[b]	*tdh*[c]	*trh*[c]	GS-PCR *toxRS/new*[d]	GS-PCR ORF8[d]	Riboprinting DuPont ID	Riboprinting Ribogroup[e]
Clinical	V96-110	O3:K6	1996	+	−	+	+	<none>	172-48-s-3
	V96-178	O3:K6	1996	+	−	+	+	DUP-6626	172-48-s-3
	V96-223	O3:K6	1996	+	−	+	+	DUP-6626	172-48-s-3
	V97-19	O3:K6	1997	+	−	+	+	DUP-6626	172-54-s-4
	V97-49	O3:K6	1997	+	−	+	+	DUP-6626	172-48-s-3
	V97-204	O3:K6	1997	+	−	+	+	DUP-6626	172-48-s-3
	V98-10	O3:K6	1998	+	−	+	+	DUP-6626	172-48-s-1
	V98-290	O3:K6	1998	+	−	+	+	DUP-6626	172-48-s-3
	V98-324	O3:K6	1998	+	−	+	+	DUP-6626	172-48-s-3
	V99-38	O3:K6	1999	+	−	+	+	DUP-6626	172-48-s-3
	V99-107	O3:K6	1999	+	−	+	+	DUP-6626	172-48-s-3
	V99-205	O3:K6	1999	+	−	+	+	DUP-6626	172-48-s-3
	V00-76	O3:K6	2000	+	−	+	+	DUP-6626	172-48-s-3
	V00-145	O3:K6	2000	+	−	+	+	DUP-6626	172-48-s-3
	V00-161	O3:K6	2000	+	−	+	+	DUP-6626	172-48-s-3
	V01-38	O3:K6	2001	+	−	+	+	DUP-6626	172-48-s-3
	V01-141	O3:K6	2001	+	−	+	+	DUP-6626	172-48-s-3
	V01-151	O3:K6	2001	+	−	+	+	DUP-6626	172-48-s-3
	V02-21	O3:K6	2002	+	−	+	+	DUP-6626	172-48-s-1
	V02-36	O3:K6	2002	+	−	+	+	DUP-6626	172-48-s-1
	V02-64	O3:K6	2002	+	−	+	+	DUP-6626	172-48-s-3
	V02-106	O3:K6	2002	+	−	+	+	<none>	172-48-s-4
	V02-123	O3:K6	2002	+	−	+	+	DUP-6626	172-48-s-3
	V02-207	O3:K6	2002	+	−	+	+	DUP-6626	172-48-s-3
	V02-279	O3:K6	2002	+	−	+	+	DUP-6626	172-48-s-3
	V03-80	O3:K6	2003	+	−	+	+	DUP-6626	172-48-s-1
	V03-108	O3:K6	2003	+	−	+	+	DUP-6626	172-48-s-3
	V03-159	O3:K6	2003	+	−	+	+	DUP-6626	172-56-s-8
Environment	V19	O3:K6	1999	−	−	−	−	<none>	172-58-s-1
	V37	O3:K6	1999	−	−	−	−	<none>	172-58-s-2
	V71	O3:K6	1999	−	−	−	−	<none>	172-58-s-3
	V237	O3:K6	2000	−	−	−	−	<none>	172-58-s-4
	V238	O3:K6	2000	−	−	−	−	<none>	172-58-s-5
	V282	O3:K6	2003	−	−	−	−	<none>	172-58-s-5

[a] All strains were isolated in Tokyo, Japan.
[b] Year of isolation.
[c] The presence of these genes were determined by the PCR as described previously (Okura et al., 2003).
[d] Determined by the group-specific PCR for the newly emerged O3:K6 strains, performed as described previously (Okura et al., 2003).
[e] Ribogroups were designated such that identical riboprint patterns are grouped into the same ribogroup.

accession numbers BA000031 and BA000032 (Fig. 1). PCR primers were designed from sequences flanking the respective loci (Table 2).

2.6. MLVA typing

Chromosomal DNA was extracted and purified from overnight cultures by phenol-chloroform extraction and ethanol precipitation according to the method of Murray and Thompson (1980).

Primers were designed for the amplification and sequencing of the target repeat region (Table 2) to verify that the observed differences were due to variability in the tandem repeat region and not other genetic characteristics. Each 50 μl PCR mixture contained 5 μl of 10×PCR buffer, 4 μl each deoxyribonucleotide, 5 μM of each primer, 0.25 μl of *Taq* DNA polymerase (Takara Bio Inc.), and 1 μl of DNA template. The samples were placed on a GeneAmp PCR System 9700 (Applied Biosystems, Foster City, Calif.) and the temperature was raised to 94 °C for 5 min, followed by 25 cycles of 94 °C for 30 s, 60 °C for 30 s, and 72 °C for 60 s. The final hold was for 7 min at 72 °C. All steps in the PCR thermal cycling program were identical for the 7 primer pairs, except for annealing temperatures (given in Table 2). The PCR products were then purified by polyethyleneglycol precipitation (Sambrook et al., 1989).

The forward and reverse strands of the PCR products were sequenced using an ABI PRISM 310 Genetic Analyzer (Applied Biosystems) and BigDye Terminator Cycle Sequencing kit (Applied Biosystems). Contigs were created using the base calling and fragment assembling software programs, GENETYX/ATSQ (Software Development, Tokyo, Japan) and the numbers of repeats in aligned sequences were counted. The resulting data were imported back into BioNumerics software version 4.0 (Applied-Maths, Kortrijk, Belgium) for use clustering analysis with the categorical coefficient and Ward clustering parameter. Use of the categorical coefficient implies that the character states are considered unordered. The

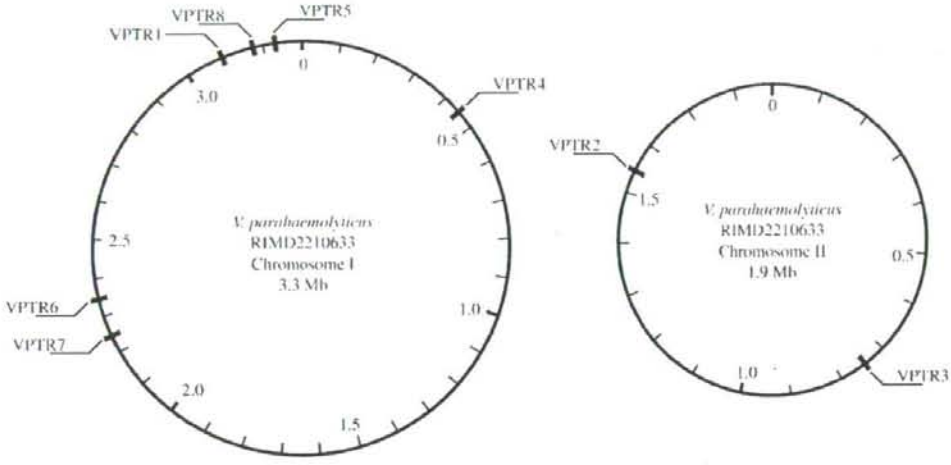

Fig. 1. VNTR maker locations within the physical map of the *V. parahaemolyticus* RIMD2210633 genome. Positions are given with reference to predicted origin of replication (set as position 0).

same weight is given to a large or a small number of differences in the number of repeats at any locus. The information index or Nei's diversity index (D) was calculated for each markers as $1-\Sigma(\text{allele frequency})^2$.

3. Results

The serotypes, virulence attributes, the results of GS-PCR for *toxRS* and ORF8, ribotyping and the sources of the 34 tested *V. parahaemolyticus* strains are shown in Table 1. PCR analysis confirmed the presence of *tdh* and the absence of *trh* in all 28 clinical strains of *V. parahaemolyticus* serotype O3:K6, while all 6 environmental strains of *V. parahaemolyticus* serotype O3:K6 lacked both *tdh* and *trh*. In addition, all 28 clinical strains were confirmed to be pandemic strains by the GS-PCR assay for *toxRS* and the ORF8 PCR assay which detects the presence of the f237 phage (Nasu et al., 2000). On the other hand, all 6 environmental strains were distinguished as nonpandemic strains by these PCR assays.

3.1. Automated ribotyping

Riboprint patterns generated for all 34 strains of *V. parahaemolyticus* O3:K6 using *Eco*RI (Table 1) showed that among the 28 clinical strains, 26 strains were identified as DuPont ID 6626 (DUP-6626; *V. parahaemolyticus*). Two

Table 2
Characteristics of the VNTR locus in *V. parahaemolyticus* and primers for MLVA

Locus	Repeat motif	Repeat times[a]	Function	Diversity[b]	Primer	Primer sequence (5′–3′)	Annealing temperature (°C)	Product size (bp)
VPTR1	ATAGAG	28	hypothetical protein	0.91	VPTR1-F	TAACAACGCAAGCTTGCAACG	60	255
					VPTR1-R	TCATTCTCGCCACATAACTCAGC		
VPTR2	CAGCAA	28	hypothetical protein	0.90	VPTR2-F	GTTACCAAACTGGCGATTACGAAG	60	615
					VPTR2-R	CGGAATTCAGGATCATCCTGAT		
VPTR3	ATCTGT	6	putative collagenase	0.35	VPTR3-F	CGCCAGTAATTCGACTCATGC	60	333
					VPTR3-R	AAGACTGTTCCCGTCGCTGA		
VPTR4	TGTGTC	7	putative hemolysin	0.43	VPTR4-F	AAACGTCTCGACATCTGGATCA	61	229
					VPTR4-R	TGTTTGGCTATGTAACCGCTCA		
VPTR5	CTCAAA	7	Non-coding region	0.56	VPTR5-F	GCTGGATTGCTGCGAGTAAGA	60	202
					VPTR5-R	AACTCAAGGGCTGCTTCGG		
VPTR6	GCTCTG	17	hypothetical protein	0.79	VPTR6-F	TGTCGATGGTGTTCTGTTCCA	60	312
					VPTR6-R	CTTGACTTGCTCGCTCAGGAG		
VPTR7	CTGCTC	6	hypothetical protein	0.38	VPTR7-F	CAACAGTTCTGCTCTAATCTTCCG	56	221
					VPTR7-R	CAAAGGTGTTACTTGTTCCAGACG		
VPTR8	CTTCTG	7	Cell division protein	0.44	VPTR8-F	ACATCGGCAATGAGCAGTTG	60	306
					VPTR8-R	AAGAGGTTGCTGAGCAAGCG		

[a] Numbers of tandem repeats were counted using the genome sequence of *V. parahaemolyticus* RIMD2210633 (Makino et al., 2003).
[b] Diversity is based on Nei's marker diversity, which is $1-\Sigma(\text{allele frequency})^2$.

strains not identified as DUP-6626, V96-110 and V02-106, showed similarities with DUP-6626 of 84% and 74%, respectively (Table 1). The majority (22 strains) of the 28 clinical strains were grouped in ribogroup 172-48-s-3 (average internal similarity, 95.9%), and 4 strains in ribogroup 172-48-s-1 had an average internal similarity 97.5%. Ribogroup 172-48-s-3 has similarity of 93%, and 172-48-s-1, 91%, with DUP-6626. All the environmental strains had no DuPont ID (Table 1).

3.2. PFGE profiles

In this study, PFGE was carried out with *Not* I. Previous experiments indicated that pandemic O3:K6 clones show similar PFGE patterns (Arakawa et al., 1999; Chowdhury et al., 2000; Yeung et al., 2002). In this study, obvious distinction between clinical and environmental strains was noted (Fig. 2). Furthermore, clinical O3:K6 group strains had highly similar PFGE patterns; all pandemic strains tested in this study displayed PFGE pattern A, except for the isolates V00-76, V00-145, V00-161, V02-21 and V02-36, which were internally identical and showed small one-band differences from the pattern A PFGE profile (PFGE pattern B). Three strains, V01-141, V01-151, and V02-207, were untypeable producing only a smear of bands on the gels. This is in accordance with previous studies (Marshall et al., 1999; Yeung et al., 2002) and suggests that the utility of PFGE for differentiating *V. parahaemolyticus*

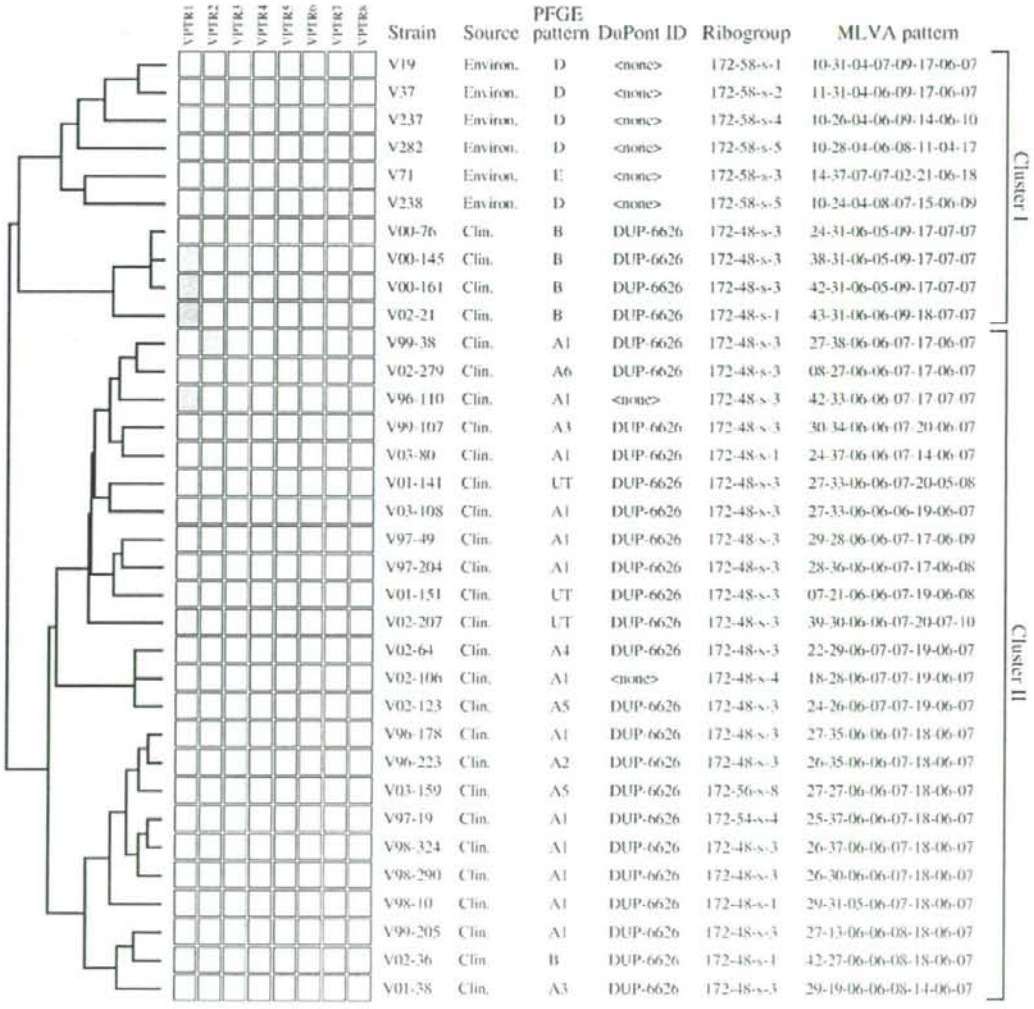

Fig. 2. The dendrogram of all the MLVA-typed *V. parahaemolyticus* O3:K6 strains. The frequencies of tandem repeats of each locus were visualized by the grayscale matrices (the color density indicates the frequency of each tandem repeats). The PFGE profile and DuPont ID generated from ribotyping are also shown. Ribogroups were designated such that identical riboprint patterns were grouped into the same ribogroup. Abbreviations: <none>, No corresponded DuPont ID; UT, untypeable.

Table 3
The number of tandem repeats of the *V. parahaemolyticus* strains used in this study

		Repeat times (Repeat motif)							
		VPTR1	VPTR2	VPTR3	VPTR4	VPTR5	VPTR6	VPTR7	VPTR8
Source	Strains	(ATAGAG)	(CAGCAA)	(ATCTGT)	(TGTGTC)	(CTCAAA)	(GCTCTG)	(CTGCTC)	(CTTCTG)
Clinical	V96-110	42	33	6	6	7	17	7	7
	V96-178	27	35	6	6	7	18	6	7
	V96-223	26	35	6	6	7	18	6	7
	V97-19	25	37	6	6	7	18	6	7
	V97-49	29	28	6	6	7	17	6	9
	V97-204	28	36	6	6	7	17	6	8
	V98-10	29	31	5	6	7	18	6	7
	V98-290	26	30	6	6	7	18	6	7
	V98-324	26	37	6	6	7	18	6	7
	V99-38	27	38	6	6	7	17	6	7
	V99-107	30	34	6	6	7	20	6	7
	V99-205	27	13	6	6	8	18	6	7
	V00-76	24	31	6	5	9	17	7	7
	V00-145	38	31	6	5	9	17	7	7
	V00-161	42	31	6	5	9	17	7	7
	V01-38	29	19	6	6	8	14	6	7
	V01-141	27	33	6	6	7	20	5	8
	V01-151	7	21	6	6	7	19	6	8
	V02-21	43	31	6	6	9	18	7	7
	V02-36	42	27	6	6	8	18	6	7
	V02-64	18	29	6	7	7	19	6	7
	V02-106	18	28	6	7	7	19	6	7
	V02-123	24	26	6	7	7	19	6	7
	V02-207	39	30	6	6	7	20	7	10
	V02-279	8	27	6	6	7	17	6	7
	V03-80	24	37	6	6	7	14	6	7
	V03-108	27	33	6	6	6	19	6	7
	V03-159	27	27	6	6	7	18	6	7
Environment	V19	10	31	4	7	9	17	6	7
	V37	11	31	4	6	9	17	6	7
	V71	14	37	7	7	2	21	6	18
	V237	10	26	4	6	9	14	6	10
	V238	10	24	4	8	7	15	6	9
	V282	10	28	4	6	8	11	4	17

might be limited by some of isolates untypeable due to DNA degradation.

3.3. PCR amplification and sequence analysis of potential VNTRs

A total of eight VNTR loci were analyzed in the *V. parahaemolyticus* genome, which consists of two circular chromosomes; six VNTRs were localized on chromosome I, and two were localized on chromosome II (Fig. 1). All eight VNTR loci were successfully amplified, and sufficient variability was confirmed in the eight VNTR loci by sequencing. We found that all eight loci had multiple alleles with substantial variability. In all cases, the size variation observed among PCR products was attributable to the number of TRs.

The VNTRs loci displayed a wide range of polymorphisms in the O3:K6 strains, with the VPTR1 and VPTR2 being the most polymorphic (Table 3). Among 28 clinical strains, VPTR1 had 18 different alleles, and VPTR2 had 16, VPTR6 had 5, VPTR5 and VPTR8 each had 4, VPTR4 and VPTR7 each had 3, and VPTR3 had only 2. The Nei's diversity index (*D*) is based on the number of alleles and the allele frequency and provides a better measure of discriminatory power than allele number; *D* values for VNTR markers in this study ranged from 0.35 for VPTR3 to 0.91 for VPTR1. VNTR analysis showed a high degree of discrimination of the O3:K6 strains.

3.4. MLVA dendrogram

The extent of genetic diversity among the tested strains based on the MLVA dendrogram revealed that each strain has a distinct profile; that is, 34 strains produced 34 patterns (Fig. 2). Only minor discrepancies were noted between the cluster pattern profiles generated by MVLA and the PFGE (Fig. 2). In MLVA analysis, two main groups, denoted as groups I and II, each were comprised of smaller groups or individual isolates. Cluster I contained all environmental O3:K6 strains and 6 pandemic O3:K6 strains. Cluster II contained the remaining pandemic O3:K6 strains. Closer inspection of cluster I, however, revealed that the pandemic O3:K6 isolates in this

cluster (V00-76, V00-145, V00-161, V02-21) in MLVA had distinct,one-band differences from the major group of the pandemic O3:K6 strains identified by PFGE (data not shown). On the other hand, the majority of strains that clustered together in PFGE produced distinct VNTR profiles, suggesting that distinct populations of *V. parahaemolyticus* serotype O3:K6 strains may have circulated during sporadic cases or in outbreaks in Tokyo during the period from 1996 to 2003. The lack of multiple isolates from the same outbreak did, however, prevent a through analysis of isolate populations.

4. Discussion

The main finding of this study was the high discrimination power of MLVA for the pandemic serotype O3:K6 strains of *V. parahaemolyticus*. All 28 of pandemic serotype O3:K6 strains tested here could be discriminated as individual strains (28 different MLVA profiles, Fig. 2). This is important since no other available typing method provides high-resolution discrimination among pandemic serotype O3:K6 strains. Previous studies using molecular analysis of O3:K6 isolates collected recently from several countries had suggested the genetic homogeneity of O3:K6 (Arakawa et al., 1999; Chowdhury et al., 2000; Matsumoto et al., 2000). The genetic homogeneity of these newly isolated O3:K6 strains were also confirmed by GS-PCR, ribotyping, and PFGE in this study. Although the clinical strains used in this study were isolated from different outbreaks or from sporadic cases during period from 1996 to 2003 in Tokyo, almost all were shown to be identical by these methods (Table 1, Fig. 2), supporting the view of previous studies that pandemic strains might have originated from the same clone (Chowdhury et al., 2000; Okuda et al., 1997). However, our MLVA results showed a high resolution for these pandemic strains, indicating substantial genetic heterogeneity at the VNTR loci among pandemic *V. parahaemolyticus* O3:K6 strains. The finding of great diversity within the small set of *V. parahaemolyticus* O3:K6 strains studied here suggests that there is still a great deal of unsampled *V. parahaemolyticus* O3:K6 diversity to be discovered. One potential concern is that VNTRs evolve so rapidly that multiple MLVA types emerge during outbreak or cultural transfers. A number of studies, however, have revealed that the composition of the VNTR loci is relatively stable and does not change even after prolonged storage or subculture in laboratory settings (Adair et al., 2000; Keim et al., 2000; Sabat et al., 2003; Truman et al., 2004). In this study, we have not tested the stability and heterogeneity within the bacterial population after extensive subculturing of individual colonies of *V. parahaemolyticus*. Thus, further studies on cultural stability and larger collections from various origins including outbreak strains are necessary to validate the application of VNTRs for the characterization of *V. parahaemolyticus*.

The functions of VNTRs used for MLVA typing in this study remain unknown, and the relationships between VNTRs and potential mechanisms for metabolic regulation as well as antigenic variation and environmental adaptation should be further examined. The VNTR loci analyzed here are widely distributed across chromosome I and II of RIMD2210633 (Fig. 1). With the exception of VPTR5, which is located in a non-coding region, VNTRs analyzed here are all located in open reading frame regions. The repeat units in the VNTRs studied in this study were all 3-bp multiples, indicating that variation in the number of repeats in these genes results in altered amino acid sequence, but not in inactivation of genes due to frame shifting. VPTR1, VPTR2, VPTR6, and VPTR7 are located in open reading frames that hypothetically codes for proteins. Allele states of the VPTR1 and VPTR2 loci are highly variable, having 18 and 16 alleles respectively. VPTR3 is located in an open reading frame that codes for the putative collagenase gene. Collagenase digests collagen, affecting the basic structure of membranes in eucaryotic cells. Studies in *V. parahaemolyticus* and *V. cholerae* have shown that collagenase activity may play a role on the virulence and be a factor in host infection and pathogenesis. Apparently, variation in VPTR3 for this gene is limited, and clinical strains, except for V98-10, have 6 repeats, indicating the essential role of putative collagenase gene in the bacterial cell. VPTR4 is located in an open reading frame that codes for the putative hemolysin gene. Pathogenicity of *V. parahaemolyticus* has been correlated to well-characterized hemolysin, TDH and TRH (Honda and Iida, 1993; Naim et al., 2001). Thermolabile direct hemolysin (TLH) (Taniguchi et al., 1990) and lectin-dependent hemolysin (LDH) (Shinoda et al., 1991) have also been reported as the virulence factors of this bacterium. However, the putative hemolysin gene which includes VPTR4 is apparently different from the above hemolysin genes. Since both clinical and environmental strains of *V. parahaemolyticus* have this gene with variation in VPTR4, these genes do not to seem to be key to the virulence of this organism. Examination of the observed allelic differences of these genes among pandemic strains and the relationship to virulence or physiological differences will be interesting for future studies.

In this study, we have shown that MLVA is a valuable typing technique for characterizing recently emerged and highly homogeneous pandemic strains of *V. parahaemolyticus* serotype O3:K6. The data presented here demonstrate the utility of this approach for individual strain identification. Although MLVA loci in pandemic O3:K6 strains seem to mutate too rapidly to be useful in determining global phylogenetic relationships, they are useful for strain identification and may identify rapidly evolving polymorphisms that are useful for discriminating very closely related strains, such as *V. parahaemolyticus* serotype O3:K6 strains. In addition to high resolution power, MLVA is a simple and rapid method, which can be used to produce strain profiles that are easily exchanged electronically via the BioNumerics database as character strings. In this study, we sequenced VPTR1 to VPTR8 amplicons to verify PCR specificity and to confirm that any observed length polymorphisms were due solely to variation in VNTR copy number. However, for practical purposes, sequencing will not be necessary and this method can be further improved by using primers tagged with multiple fluorescent dyes, allowing accurate sizing of amplicons by automated DNA sequencer analysis. This method therefore gives fast, discriminative, and reproducible results for epidemiological surveillance of *V. parahaemolyticus* pandemic strains.

Acknowledgements

This work was partly supported by the National Food Research Institute of Japan (project: Development of evaluation and management methods for supply of safe, reliable and functional food and farm produce) and Japanese Ministry of Health, Labour and Welfare (H19-011).

The authors thank for Tatsuya Ishikawa for MLVA data analyses.

References

Adair, D.M., Worsham, P.L., Hill, K.K., Klevytska, A.M., Jackson, P.J., Friedlander, A.M., Keim, P., 2000. Diversity in a variable-number tandem repeat from *Yersinia pestis*. J. Clin. Microbiol. 38, 1516–1519.

Arakawa, E., Murase, T., Shimada, T., Okitsu, T., Yamai, S., Watanabe, H., 1999. Emergence and prevalence of a novel *Vibrio parahaemolyticus* O3:K6 clone in Japan. Jpn. J. Infect. Dis. 52, 246–247.

Bag, P.K., Nandi, S., Bhadra, R.K., Ramamurthy, T., Bhattacharya, S.K., Nishibuchi, M., Hamabata, T., Yamasaki, S., Takeda, Y., Nair, G.B., 1999. Clonal diversity among recently emerged strains of *Vibrio parahaemolyticus* O3:K6 associated with pandemic spread. J. Clin. Microbiol. 37, 2354–2357.

Benson, G., 1999. Tandem repeats finder: a program to analysis DNA sequences. Nucleic Acids Res. 27, 573–580.

Centers for Disease Control and Prevention, 1999. Outbreak of *Vibrio parahaemolyticus* infection associated with eating raw oysters and clams harvested from Long Island Sound — Connecticut, New Jersey, and New York, 1998. Morbid. Mortal. Weekly Rep. 48, 48–51.

Chowdhury, N.R., Stine, O.C., Morris, J.G., Nair, G.B., 2004. Assessment of evolution of pandemic *Vibrio parahaemolyticus* by multilocus sequence typing. J. Clin. Microbiol. 42, 1280–1282.

Chowdhury, N.R., Chakraborty, S., Ramamurthy, T., Nishibuchi, M., Yamasaki, S., Takeda, Y., Nair, G.B., 2000. Molecular evidence of clonal *Vibrio parahaemolyticus* pandemic strains. Emerg. Infect. Dis. 6, 631–636.

DePaola, A., Ulaszek, J., Kaysner, C.A., Tenge, B.J., Nordstrom, J.L., Wells, J., Puhr, N., Gendel, S.M., 2003. Molecular, serological, and virulence characteristics of *Vibrio parahaemolyticus* isolated from environmental, food, and clinical sources in North America and Asia. Appl. Environ. Microbiol. 69, 3999–4005.

Gendel, S.M., Ulaszek, J., Nishibuchi, M., DePaola, A., 2001. Automated ribotyping differentiates *Vibrio parahaemolyticus* O3:K6 strains associated with a Texas outbreak from other clinical strains. J. Food Prot. 64, 1617–1620.

Hara-Kudo, Y., Sugiyama, K., Nishibuchi, M., Chowdhury, A., Yatsuyanagi, J., Ohtomo, Y., Saito, A., Nagano, H., Nishina, T., Nakagawa, H., Konuma, H., Miyahara, M., Kumagai, S., 2003. Prevalence of pandemic thermostable direct hemolysin-producing *Vibrio parahaemolyticus* O3:K6 in seafood and the coastal environment in Japan. Appl. Environ. Microbiol. 69, 3883–3891.

Honda, T., Iida, T., 1993. The pathogenicity of *Vibrio parahaemolyticus* and the role of the thermostable direct hemolysin and related hemolysins. Rev. Med. Microbiol. 4, 106–113.

Keim, P., Price, L.B., Klevytska, A.M., Smith, K.L., Schupp, J.M., Okinaka, R., Jackson, P.J., Hugh-Jones, M.E., 2000. Multiple-locus variable-number tandem repeat analysis reveals genetic relationships within *Bacillus anthracis*. J. Bacteriol. 182, 2928–2936.

Lindstedt, B.A., Vardund, T., Kapperud, G., 2004a. Multiple-locus variable-number tandem-repeat analysis of *Escherichia coli* O157 using PCR multiplexing and multi-colored capillary electrophoresis. J. Microbiol. Methods 58, 213–222.

Lindstedt, B.A., Vardund, T., Aas, L., Kapperud, G., 2004b. Multiple-locus variable-number tandem-repeats analysis of *Salmonella enterica* subsp. *enterica* serovar Typhimurium using PCR multiplexing and multicolor capillary electrophoresis. J. Microbiol. Methods 59, 163–172.

Makino, K., Oshima, K., Kurokawa, K., Yokoyama, K., Uda, T., Tagomori, K., Iijima, Y., Najima, M., Nakano, M., Yamashita, A., Kubota, Y., Kimura, S., Yasunaga, T., Honda, T., Shinagawa, H., Hattori, M., Iida, T., 2003. Genomic sequence of *Vibrio parahaemolyticus*: a pathogenic mechanism distinct from that of *V. cholerae*. Lancet 361, 743–749.

Marshall, S., Clark, C.G., Wang, G., Mulvey, M., Kelly, M.T., Johnson, W.M., 1999. Comparison of molecular methods for typing *Vibrio parahaemolyticus*. J. Clin. Microbiol. 37, 2473–2478.

Matsumoto, C., Okuda, J., Ishibashi, M., Iwanaga, M., Garg, P., Rammamurthy, T., Wong, H., DePaola, A., Kim, Y.B., Albert, M.J., Nishibuchi, M., 2000. Pandemic spread of an O3:K6 clone of *Vibrio parahaemolyticus* and emergence of related strains evidenced by arbitrarily primed PCR and *toxRS* sequence analyses. J. Clin. Microbiol. 38, 578–585.

Metzgar, D., Thomas, E., Davis, C., Field, D., Wills, C., 2001. The microsatellites of *Escherichia coli*: rapidly evolving repetitive DNAs in a non-pathogenic prokaryote. Mol. Microbiol. 39, 183–190.

Murray, M., G., Thompson, W.F., 1980. Rapid isolation of high molecular weight plant DNA. Nucl. Acids Res. 8, 4321–4325.

Naim, R., Yanagihara, I., Iida, T., Honda, T., 2001. *Vibrio parahaemolyticus* thermostable direct hemolysin can induce an apoptotic cell death in Rat-1 cells from inside and outside of the cells. FEMS Microbiol. Lett. 195, 237–244.

Nasu, H., Iida, T., Sugahara, T., Yamaichi, Y., Park, K., Yokoyama, K., Makino, K., Shinagawa, H., Honda, T., 2000. A filamentous phage associated with recent pandemic *Vibrio parahaemolyticus* O3:K6 strains. J. Clin. Microbiol. 38, 2156–2161.

Noller, A.C., McEllistrem, M.C., Pacheco, A.G.F., Boxrud, D.J., Harrison, L.H., 2003. Multilocus variable-number tandem repeat analysis distinguishes outbreak and sporadic *Escherichia coli* O157:H7 isolates. J. Clin. Microbiol. 41, 5389–5397.

Okuda, J., Ishibashi, M., Hayakawa, E., Nishino, T., Takeda, Y., Mukhopadhyay, A.K., Garg, S., Bhattacharya, S.K., Nair, G.B., Nishibuchi, M., 1997. Emergence of a unique O3:K6 clone of *Vibrio parahaemolyticus* in Calcutta, India, and isolation of strains from the same clonal group from Southeast Asian travelers arriving in Japan. J. Clin. Microbiol. 35, 3150–3155.

Okura, M., Osawa, R., Iguchi, A., Arakawa, E., Terajima, J., Watanabe, H., 2003. Genotypic analyses of *Vibrio parahaemolyticus* and development of a pandemic group-specific multiplex PCR assay. J. Clin. Microbiol. 41, 4676–4682.

Onteniente, L., Brisse, S., Tassios, P.T., Vergnaud, G., 2003. Evaluation of polymorphisms associated with tandem repeats for *Pseudomonas aeruginosa* strain typing. J. Clin. Microbiol. 41, 4991–4997.

Sabat, A., Krzyszton-Russjan, J., Strzalka, W., Filipek, R., Kosowska, K., Hryniewicz, W., Travis, J., Potempal, J., 2003. New method for typing *Staphylococcus aureus* strains: multiple-locus variable-number tandem repeat analysis of polymorphism and genetic relationships of clinical isolates. J. Clin. Microbiol. 41, 1801–1804.

Sambrook, J.E., Fritsch, F., Maniatis, T.S., 1989. Molecular cloning: A Laboratory Manual, 2nd edn. Cold Spring Harbor Laboratory, Cold Spring Harbor, New York.

Shinoda, S., Matsuoka, H., Tsuchie, T., Miyoshi, S., Yamamoto, S., Taniguchi, H., Mizuguchi, Y., 1991. Purification and characterization of a lecithin-dependent hemolysin from *Escherichia coli* transformed by a *Vibrio parahaemolyticus* gene. J. Gen. Microbiol. 137, 2705–2711.

Sreenu, V.A., Alevoor, V., Nagaraju, J., Nagarajaram, H.A., 2003. MICdb: database of prokaryotic microsatellites. Nucleic Acids Res. 31, 106–108.

Taniguchi, H., Kubomura, S., Hirano, H., Mizue, K., Ogawa, M., Mizuguchi, Y., 1990. Cloning and characterization of a gene encoding a new thermostable hemolysin from *Vibrio parahaemolyticus*. FEMS Microbiol. Lett. 67, 339–345.

Truman, R., Fontes, A.B., de Miranda, A.B., Suffys, P., Gillis, T., 2004. Genotypic variation and stability of for variable-number tandem repeats and their suitability for discriminating strains of *Mycobacterium leprae*. J. Clin. Microbiol. 42, 2558–2565.

Wong, H.C., Liu, S.H., Wang, T.K., Lee, C.L., Chiou, C.S., Liu, D.P., Nishibuchi, M., Lee, B.K., 2000. Characteristics of Vibrio parahaemolyticus O3:K6 from Asia. Appl. Environ. Microbiol. 66, 3981–3986.

Yeung, P.S.M., Hayes, M.C., DePaola, A., Kaysner, C.A., Kornstein, L., Boor, K.J., 2002. Comparative phenotypic, molecular, and virulence characterization of *Vibrio parahaemolyticus* O3:K6 isolates. Appl. Environ. Microbiol. 68, 2901–2909.

J Ind Microbiol Biotechnol (2007) 34:685–688
DOI 10.1007/s10295-007-0231-7

SHORT COMMUNICATION

Visualization of yeast single-cells on fabric surface with a fluorescent glucose and their isolation for culture

Kohtaro Fujioka · Philip Geis · Mikako Saito · Hideaki Matsuoka

Received: 25 March 2007 / Accepted: 20 May 2007 / Published online: 14 June 2007

Abstract An ultra-deep focusing range (UDF) fluorescent microscope system has been combined with a micromanipulation system to develop a viable cell detection-identification system applicable to microbes on environmental surfaces and products. *Candida albicans* yeast cells on a fabric sample surface were viably stained with a fluorescent glucose derivative, 2-[*N*-(7-nitrobenz-2-oxa-1,3-diazol-4-yl)amino]-2-deoxy glucose (2-NBDG) and detected with a UDF fluorescent microscope. Visualized single-cells of *C. albicans* were picked in a glass microcapillary and transferred onto an agar medium. After the culture, the colony was assayed for DNA sequence to identify the isolate. This demonstrates a potential application to the study of unknown environmental microorganisms.

Keywords Ultra-deep focusing range (UDF) fluorescent microscope · Single-cell manipulation · Fluorescent glucose derivative · Viable cell imaging

K. Fujioka
Kobe Technical Center, Procter & Gamble Far East, Inc., 17, Koyo-cho Naka 1-Chome, Higashinada-ku, Kobe 658-0032, Japan

K. Fujioka · M. Saito · H. Matsuoka (✉)
Department of Biotechnology and Life Science, Tokyo University of Agriculture and Technology, Koganei, Tokyo 184-8588, Japan
e-mail: bio-func@cc.tuat.ac.jp

P. Geis
Sharon Woods Technical Center, The Procter & Gamble Co., 11530 Reed Hartman Highway, Cincinnati, OH 45242, USA

Introduction

Quantitative and qualitative analyses of environmental microorganisms have been attempted with various methods and approaches [2, 3, 7, 13, 15]. Where effective, these usually require days to obtain the results and fail to connect the visual to microbial species. Currently, urgent needs exist in the detection of food pathogens in cooking environment [11, 17] and microbial growth in damp garments after the laundry washing process [10, 14]. To meet these needs, we have recently developed a ultra-deep focusing range (UDF) fluorescent microscope system and applied it successfully to the evaluation of microbial cell removal from fabrics [4], and to the automatic mapping of viable microbial cells being distributed in the surface layer of cotton fabrics [5]. The next step is to isolate those single-cells for their identification. Once the single-cells have been isolated, they can be cultured on an agar medium. Thus formed colonies may be used for further investigation including DNA analysis and metabolism analysis. This research demonstrates the detection of single-cells of *Candida albicans* on fabrics and their isolation for the culture.

Materials and methods

Microbial strains

Candida albicans, which is one of the key human pathogens [6, 16] and contaminants in cosmetic industry [1] was chosen as a microbial strain for this study. Seed cultures of *C. albicans* ATCC 10231 were prepared from frozen stocks from MICROBANK kit (Pro-lab Diagnostics, Toronto, Canada) and cultured in the 1/10th strength Trypticase Soy Broth (1/10 TSB) to approximately 10^6 cfu/ml. Fabric

samples used are Kanakin 3 [8]. Fabric swatches were prepared as 1.0 cm × 1.0 cm squares, wrapped with aluminum foil, autoclaved at 121°C for 15 min, and dried under sterile conditions.

Fluorescent glucose derivative treatments

Synthesis of 2-[*N*-(7-nitrobenz-2-oxa-1,3-diazol-4-yl)amino]-2-deoxy glucose (2-NBDG) was conducted following the protocol described elsewhere [18].

A 200 µl inoculum of the seed culture containing about 5×10^6 cells of *C. albicans* was inoculated onto a swatch, and the swatch was placed on Trypticase Soy Agar (TSA) plates. After incubation at 33°C for 1 h, the remaining aqueous liquid on the swatch was removed by Ultrafree-MC centrifuging treatment (6,000 rpm × 30 s). To obtain individual components amendable to microscopic observations, the centrifuged swatch was untied and dissected to individual strings with pre-sterilized tweezers. The individual fabric strings were set on a glass slide upon which a square grid has been imprinted. Approximately 2.0 ml of 0.2% agarose solution containing 12 µM 2-NBDG was prepared in molten condition at 46°C, and poured onto the reassembled fabric strings on the slide glass. The glass slide was kept in a petri-dish and incubated for 1 h at 33°C to facilitate the uptake of 2-NBDG by *C. albicans*.

Microscope and manipulation systems

After incubation, the glass slide was examined with a UDF fluorescent microscope system. The detailed components of the UDF fluorescent system are described previously [4, 5]. Ultra long distance industrial optical lenses (CFI Plan EPI SLWD 50 and 30, NIKON Co., working distance 17.0 and 24.0 mm, respectively) and a semi-automatic cell injection manipulator (InjectMan NI2, Eppendorf Co.) were integrated to assemble a cell manipulation system (Fig. 1). InjectMan NI2 was fixed on the UDF system stage with steel frames.

To prepare glass capillaries for the yeast cell manipulation, borosilicate glass tubes (BF100-78-10, diameter 1.0–0.78 mm, Sutter Instrument Co.) were pulled with a laser puller (P-2000, Sutter Instrument Co.), sterilized with anhydrous ethyl alcohol and dried in a dry oven at 50°C for 48 h. For cell manipulation, a sterile silicone tube 2 mm in diameter was connected to the capillary and to the InjectMan NI2.

DNA sequence analyses

Isolated cells were incubated on TSA plates at 33°C for 48 h to prepare sufficient cell mass for DNA sequence analyses. The harvested cells were transferred to a 1.8 mL serum tube and frozen in liquid nitrogen. Frozen cells were treated with homogenization pestle to break the cell wall. This process was repeated two times. DNA was extracted from the homogenate with E.N.Z.A. Fungal DNA Kit (Omega Bio-tek, Inc.). PCR amplification was conducted on the 26S rDNA D1/D2 regions [9] with primers NL-1(5′-CGATATCAATAAGCGGAGGAAAAG) and NL-4(5′-GGTCCGTGTTTCAAGACGG) [12] with a thermal cycler (PTC-200 Peltier Thermal Cycler, MJ Research Co.) under the conditions of 95°C × 10 s + 50°C × 60 s + 70°C × 60 s (denaturation, annealing, and extension, 30 cycles), and 72°C × 10 min (extension) . The PCR products obtained were purified with QIA quick PCR Purification Kit (QIAGEN Co.) and DNA sequence analyses were done with PRISM3100 genetic Analyzer (ABI Co.).

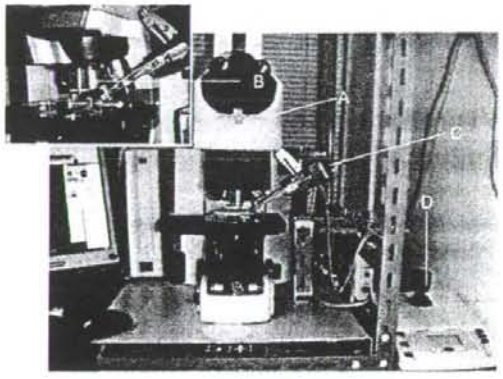

Fig. 1 A UDF fluorescent microscope system with a cell manipulation system. *A* microscope, *B* ultra long distance industrial optical lens, *C* manipulator, *D* operation module of manipulator

Results and discussion

The fluorescent images indicate viabile cells attaching on the surface of fabrics and their morphologies can be recognized (Fig. 2). Following this cell detection, a glass capillary was inserted in molten agar and placed adjacent to cells (Fig. 3a, fluorescent image). Then the cells were sucked into the capillary (Fig. 3b, c). The isolated cells were cultured as described and subjected to DNA sequence analysis at D1/D2 domain in 26S rDNA to certify that the originally inoculated strain was recovered. The gel electrophoresis band picture of the PCR product is shown in Fig. 4. A single band appeared at the same position as that obtained from the originally inoculated cells. The DNA sequence analyses data of 572 bp indicated 100% sequence matching. These indicate the clear traceability of the inoculated strain.

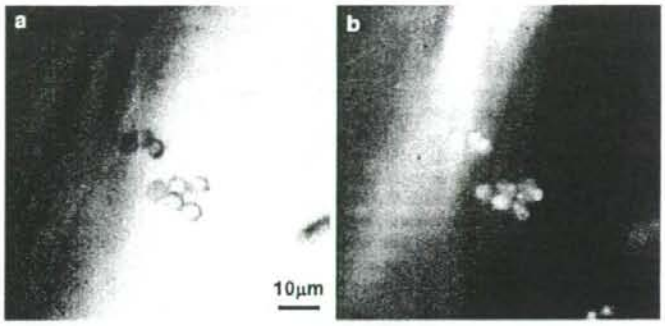

Fig. 2 Microscopic images of *Candida albicans* observed on fabric before cell isolation. **a** Optical image, **b** fluorescent image

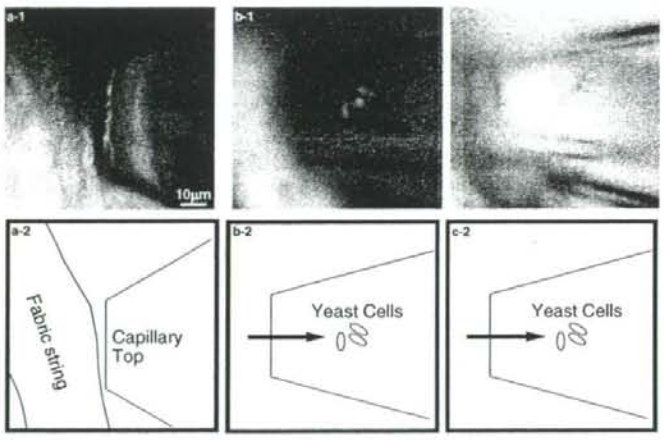

Fig. 3 Cell isolation procedure. **a** Glass capillary inserted to molten agar coating the fabric (optical image), **b**, **c** *C. albicans* cells sucked in a capillary stored in the glass capillary [optical image (**b**) and fluorescent image (**c**)]

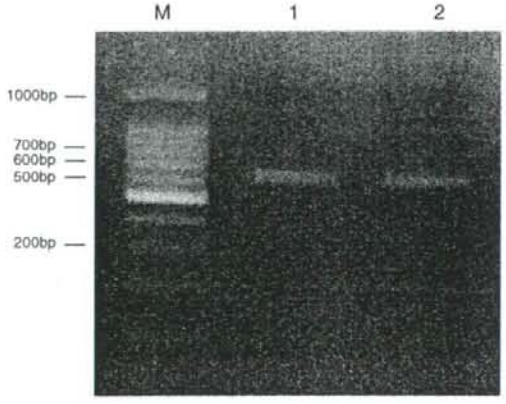

Fig. 4 Gel electrophoresis band picture of the PCR products. A total of 2% agarose, TAE Buffer, *M* Takara 100 bp ladder as a marker, *1* DNA derived from the inoculated strain, *2* DNA derived from the manipulated/isolated strain

Successful visualization and manipulation demonstrate the applicability of the present system to the detection of very low numbers of microbial cells and for their successive culture. The first is to detect viable cells rapidly and the next is to investigate them carefully depending upon the necessity.

Single-cell manipulation supporting technologies have recently gained marked progress [19, 20] and therefore the present system may be advanced to a higher throughput system in response to practical needs.

Acknowledgments This research was supported by the Microbial Visualization Community of Practice in The Procter & Gamble Company. H.M. acknowledges supports from Grant-in-aid for Scientific Research for the Promotion of Safety and Security of Foods, The Ministry of Health, Labor, and Welfare, and from CREST of Japan Science and Technology Agency.

References

1. Abedelaziz A-A, Ashour M-S (1987) Microbial contamination of hexetidine mouth wash. Zentrabl Bakteriol Mikrobiol Hyg [B] 184:262–268
2. Brown D-F, Dupont J, Dumont F, menanteau C, Pommepuy M (2004) Calibration of the impedance method for rapid quantitative estimation of *Escherichia coli* in live marine bivalve molluscs. J Appl Microbiol 4:894–902

3. Esioubu N (2006) Use of peptide nucleic acid probes for rapid detection and enumeration of viable bacteria in recreational waters and beach sand. Methods Mol Biol 345:131–140
4. Fujioka K, Kozone I, Saito M, Matsuoka H (2006) Rapid evaluation of the efficacy of microbial cell removal from fabrics. J Ind Microbiol Biotechnol 33:995–1002
5. Fujioka K, Kozone I, Saito M, Matsuoka H (2007) Automatic mapping of viable microbial cells being distributed in the surface layer of cotton fabrics. Biocontrol Sci 12(1):31–34
6. Hansson C, Jekler J, Swanbeck G (1985) *Candida albicans* infections in leg ulcers and surrounding skin after the use of ointment impregnated stockings. Acta Derm Venereol 65:424–427
7. Jimenez L (2001) Molecular diagnosis of microbial contamination in cosmetic and pharmaceutical products: a review. J AOAC Int 84:671–675
8. JIS L0803 (1998) Standard adjacent fabrics for straining of colour fastness test
9. Kurtzman C-P, Robnett C-J, (1998) Identification and phylogeny of ascomycetous yeasts from analysis of nuclear large subunit (26S) ribosomal DNA partial sequences. Antonie van Leeuwenhoek 73:331–371
10. Marples R-R, Towers A-G (1979) A laboratory model for the investigation of contact transfer of micro-organisms. J Hyg (Lond) 82:237–248
11. Nielsen P, Brumbaugh E, Kananen L (2002) Evaluation of the use of liquid dishwashing compounds to control bacteria in kitchen sponges. J AOAC Int 85:107–112
12. O'Donnell K, (1993) *Fusarium* and its near relatives. In: Reynolds DR, Taylor JW (ed) The fungal holomorph: mitotic, meiotic and pleomorphic speciation in fungal systematics. CAB International, Wallingford, pp 225–233
13. Odumeru J-A, Belvedere J (2002) Evaluation of the MicroFoss system for enumeration of total viable count, *Escherichia coli* and coliforms in ground beef. J Microbiol Methods 50:33–38
14. Patrick D-R, Findon G, Miller T-E (1997) Residual moisture determines the level of touch-contact-associated bacterial transfer following hand washing. Epidemiol Infect 119:319–325
15. Ren Z, Hsiehi Y-H (2005) Real-time determination of microbial activity of pasteurized fluid milk using a novel microrespirometer method. J AOAC Int 88:1756–1761
16. Scherer S, Magee P-T (1990) Genetics of *Candida albicans*. Microbiol Rev 54:226–241
17. Venkitanarayanan K-S, Ezeike G-O, Hung Y-C, Doyle M-P (1999) Inactivation of *Escherichia coli* O157:H7 and *Listeria monocytogenes* on plastic kitchen cutting boards by electrolyzed oxidizing water. J Food Prot 62:857–860
18. Yoshioka K, Takahashi H, Homma T, Saito M, Oh K-B, Nemoto Y, Matsuoka H (1996) A novel fluorescent derivative of glucose applicable to the assessment of glucose uptake activity of *Escherichia coli*. Biochim Biophys Acta 1289:5–9
19. Matsuoka H, Komazaki T, Mukai Y, Shibusawa M, Akane H, Chaki A, Uetake N, Saito M (2005) High throughput easy microinjection with a single-cell manipulation supporting robot. J Biotechnol 116:185–194
20. Matsuoka H, Yamada Y, Matsuoka K, Saito M (2006) High throughput microinjection technology for the single-cell analysis of BY-2 in vivo. In: Nagata T, Matsuoka K, Inzé D (eds) Tobacco BY-2 cells: from cellular dynamics to omics. Springer, Berlin, pp 339–346

Biocontrol Science, 2007, Vol. 12, No. 1, 31−34

Note

Automatic Mapping of Viable Microbial Cells Distributed in the Surface Layer of Cotton Fabrics

KOHTARO FUJIOKA[1, 2], IKUKO KOZONE[2], MIKAKO SAITO[2], AND HIDEAKI MATSUOKA[2*]

[1]*Kobe Technical Center, Procter & Gamble Far East, Inc., 17, Koyo-cho Naka 1-Chome, Higashinada-ku, Kobe 658-0032, Japan*
[2]*Department of Biotechnology and Life Science, Tokyo University of Agriculture and Technology, Koganei, Tokyo 184-8588, Japan*

Received 17 October 2006/Accepted 18 January 2007

Viable microbial cells distributed in a 130 μm thick surface layer of cotton fabrics were stained with a fluorescent glucose, 2-[*N*-(7-nitrobenz-2-oxa-1,3-diazol-4-yl)amino]-2-deoxy-D-glucose (2-NBDG), and automatically mapped with an ultra-deep focusing range microscope (UDF) system. The software of the UDF system was upgraded and the number of *Candida albicans* cells could be counted at a higher precision than before. Bacterial cells of *Pseudomonas fluorescens, Serratia marcescens*, and *Citrobacter freundii*, which were smaller than 1-2 μm, were successfully mapped for the first time. These results indicate the practical importance of the present method in the evaluation of the antibacterial properties of fabrics and the efficacy of washing.

Key words : Ultra-deep focusing range (UDF) fluorescent microscope/A fluorescent glucose/ Viable cell imaging/Cell deposition on fabrics.

Visualization *in situ* of viable microbial cells on the surface of fabrics is of practical importance and has been important for the evaluation of antibaterial properties of fabrics (JIS L1902, 2002; Borkow and Gabbay, 2004; Cen et al., 2004) and the efficacy of washing (Petrocci and Clarke, 1969; JIS L0844, 1997; ASTM E2274-03, 2004). One of the key challenges in conducting such an evaluation is to deal with the topology of fabric surfaces which is not flat at the micrometer scale but composed of many fibers to form a complex structure. Microbial cells are deposited on thin fibers or entrapped deeply between fibers. To detect these cells within a deep focusing range simultaneously, confocal microscopy (Roldán et al., 2004; Staudt et al., 2004), decomvolution microscopy (McNally et al., 1999), and other methods (Burton, 2003; Buda et al., 2005) have been proposed and in fact some models based on these principles are commercially available. However it was difficult to modify available models at a reasonable cost to fit our specific resolutional purpose. Thus we developed a novel microscopic system with an UDF system (Fujioka et al., 2006). In combination with the staining of viable cells with a fluorescent glucose derivative, 2-NBDG (Yoshioka et al., 1996; Matsuoka et al., 2003), the UDF system was found to be useful for the rapid evaluation of the efficacy of microbial cell removal (EMR) from fabrics in the specific case of *Candida albicans* microbes greater than 5 μm.

From a practical viewpoint, however, it is essential to establish a spatial resolution as high as 1-2 μm. In this study, we have critically revised the principal image processing software. As described below, the mapping of *C. albicans* has been successfully performed with much higher resolution. The mappings of bacterial cells smaller than 1-2 μm are also demonstrated.

Seed cultures of *C. albicans* ATCC10231, the environmental isolates of *Pseudomonas fluorescens*,

*Corresponding author. Tel : +81-42-388-7029, Fax : +81-42-387-1503, e-mail: mhide@cc.tuat.ac.jp

Serratia marcescens, and *Citrobacter freundii* were prepared from respective frozen stocks with MICROBANK kit (Pro-lab Diagnostics, Toronto, Canada) and cultured in 1/10 strength Trypticase Soy Broth (1/10 TSB) to approximately 10^6 cfu/ml. Fabric samples used were Kanakin 3 (JIS L0803, 1998), Cotton knit without a brightener, and Cotton 100 denim. These are differently knitted to form unique textures and certified by the Japan Spinners' Association. The fabric swatches were prepared as 1.0 cm × 1.0 cm squares, wrapped with aluminum foil, autoclaved at 121℃ for 15 min, and dried up under sterilized conditions. The synthesis of 2-NBDG was performed following the protocol described elsewhere (Yoshioka et al., 1996).

A 50 μl inoculum of the seed culture containing about 5×10^5 cells of *C. albicans* was inoculated onto each swatch, and the swatch was placed on Trypticase Soy Agar (TSA) plates. After the incubation at 33℃ for 16 h, each swatch was soaked in 9ml saline and vortexed for 5 min to remove most of the microbial cells from the each swatch. Thus we prepared swatch samples on which only small numbers of microbial cells remained. Each swatch was cut into 2 pieces (0.5 cm × 1.0 cm each). One piece (I) was used for the visualization experiment after being stained with 2-NBDG. The other piece (II) was used for the colony count assay only in the case of bacterial cells.

The conditions of 2-NBDG staining were as follows. A 400 μl aliquot of 12 μM 2-NBDG was placed on the fabric swatch piece (I). After incubation at 33℃ for 10 min, the remaining aqueous liquid was removed by Ultrafree-MC centrifuging treatment (6000 rpm × 30s). After that, a 100 μl of 30% formaldehyde (HCHO) solution was added with a pipette on the swatch and incubated at 33℃ for 1 min in order to fix the microbial cells. Immediately after that, the swatch was soaked in 9 ml saline for 5 min and centrifuged (6000 rpm × 30 s) to remove extracellular 2-NBDG. This washing with saline was repeated 2 times and microscopic observation with the UDF system was performed.

Previously we often encountered the image of a *C. albicans* cell indicated by an arrow in Fig. 1. In such a case, the single-cell emitted intense fluorescence at both ends and consequently was recognized as 2 cells in the automatic mapping. Such an image was due to a large vacuole that could hardly be stained by 2-NBDG. The increase in the spatial resolution, however, has enabled the recognition of such a case as a single-cell. Typical cases are observed at 4 positions in Fig. 2-Aa. These spots could be successfully registered as single-cells, respectively, as No. 1, 2, 5, and 8 in Fig. 2-Ab. A similar case is also observed in Fig. 2-Ba and registered as No. 5.

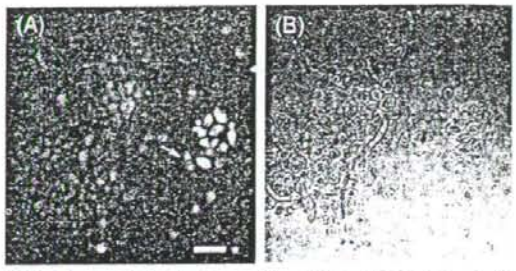

FIG. 1. Typical fluorescent pattern observed in *C. albicans* stained with 2-NBDG. (A) Fluorescent image, (B) Bright field image. Scale bar: 10 μm. The arrow indicates a typical image pattern of both ends emitting intense fluorescence. Observed with VC100×oil objective lens through BV-2A filter.

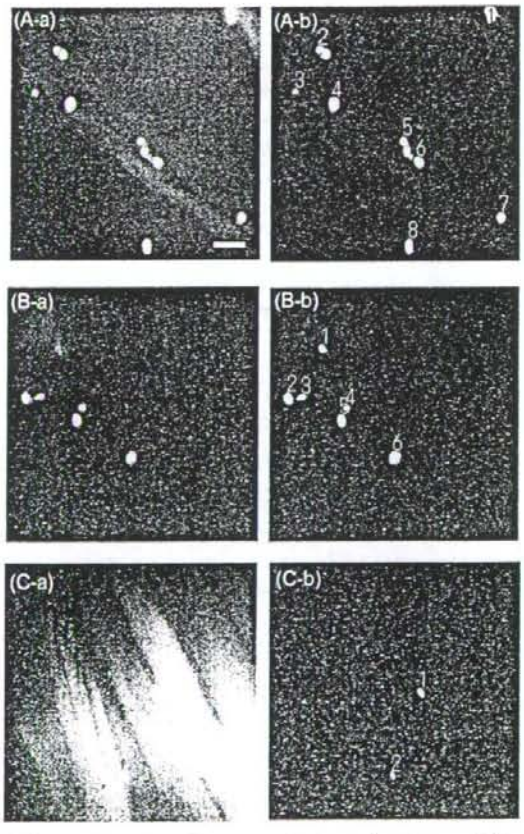

FIG. 2. Mapping of *C. albicans* in the surface layer of different cotton materials. (A) Kanakin3, (B) Cotton Knit without brightener, (C) Cotton 100 Denim. Scale bar: 10 μm.

As may be observed in the Figs. 2-Ab, 2-Bb, and 2-

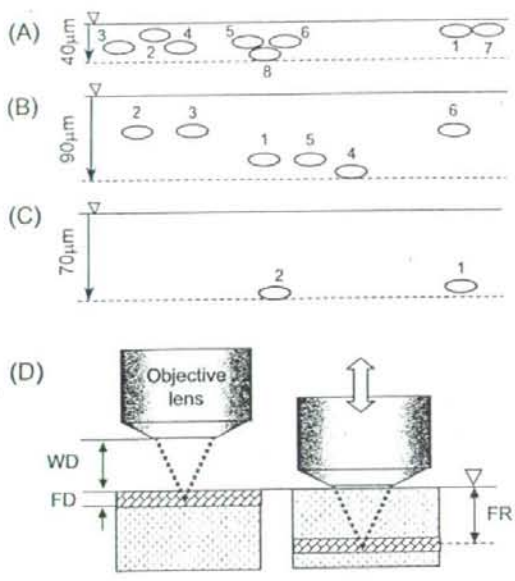

FIG. 3. Estimated depth of each cell from the fabric surface. Numbered cells in (A), (B), and (C) correspond to the numbered cells in (A), (B), and (C) of Fig.2, respectively. (D) Focusing range that can be observed simultaneously by the UDF system. ▽: Fabric surface, - - - in (A)~(C): Deepest cell level observed in respective cases, WD: Working distance (130 μm), FD: In-focus depth (a few μm), FR: Focusing Range (max 130 μm).

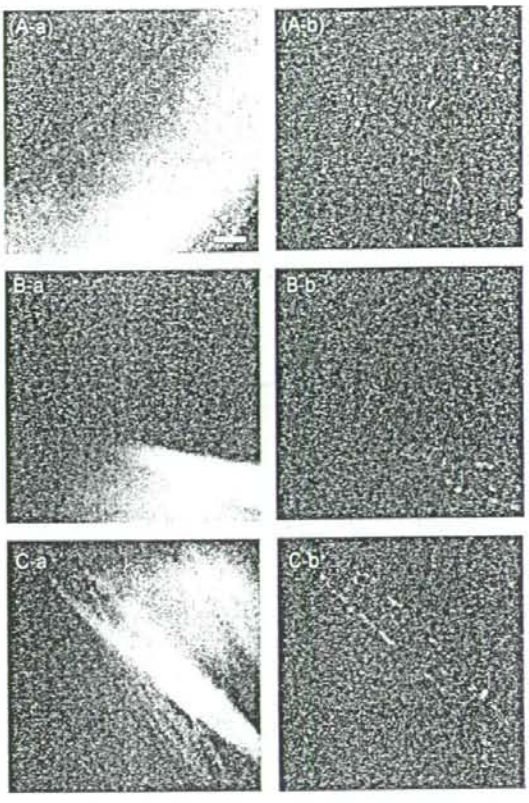

FIG. 4. Mapping of bacterial cells in the surface layer of Kanakin3. (A) *P. fluorescens*, (B) *S. marcescens*, (C) *C. freundii*. Observed with VC100×oil objective lens through BV-2A filter. Scale bar: 10 μm.

Cb, it is noticed that every fluorescent spot looks equally clear in outline and similar in size, though every cell does not necessarily exist in the same depth. The UDF system can integrate microscopic images from the surface to 130 μm depth at maximum (Fig. 3-D). Therefore the mapping data include the information of the depth of each cell. Based on these data, approximate positions of respective cells are shown in Figs. 3-A, 3-B, and 3-C. Such data are useful to estimate the degree of cell invasion into fabric matrices of different physical properties as well as their removal by washing.

Next is the automatic mapping of bacterial cells smaller than 2-3 μm. The objective lens was ×100 APO to zoom into the bacterial cell. In the case of Fig. 4-Aa, many fluorescent spots could be observed with similar fluorescent intensities. Thus every spot could be mapped as a light spot of similar size by adjusting the threshold level for the binarization at an appropriate level (Fig. 4-Ab). In the other two cases, only one cell was recognized as a light spot (Figs. 4-Ba, 4-Ca). According to the properly adjusted threshold level and the criteria for single-cell size, only this spot could be registered as a bacterial cell (Fig. 4-Bb, 4-Cb).

Practically, it is necessary to confirm the quantitative relation between the cell numbers determined by the present method and by the conventional colony count method. However, the challenge of statistics regarding sample size still remained. In fact the area that was analyzed by the present method was too small to be compared to the colony count method. This problem will be resolved by the future development of an automatic scanning system for a fabric swatch of a much larger area.

Since only one cell is detected in Fig.4-B and 4-C respectively, it may be necessary to confirm by the colony count method that bacterial cells were actually remaining on/in the fabric swatch. The other halves (swatch piece (II)) used for Fig. 4 were assayed for viable cells according to the following protocol. The swatch piece (II) was immersed in 9 ml of 1/10 TSB and vortexed for 5 min and then taken out from the 1/10 TSB. A 0.5 ml aliquot of the 1/10 TSB

(suspension A) was mixed with TSA and poured in a dish for culturing at 33℃ for 72 h. Since the cell concentration in the suspension A was thought to be markedly small, suspension A was also incubated at 33℃ for another successive 48 h to increase it. A 100 μl aliquot of the resulting suspension (suspension B) was spread on a TSA plate and incubated at 33 ℃ for 24 h to count the colony number. As a result, after the incubation, no colony growth was observed on the TSA plates of suspension A. On the other hand, some growth was observed on the plates of suspension B (Fig.4-B: 44 cfu/plate, Fig.4-C: 55 cfu/plate). This supports the idea that the amounts of the residual levels of bacteria are very low.

In conslusion, the UDF system has been upgraded so that it may count automatically the cell number of *C. albicans* as well as smaller bacterial cells at a higher precision than before. The present results suggest the importance of the further development of a practical version of the UDF system.

Acknowledgments

This research was supported by the Microbial Visualization Community of Practice of the Procter & Gamble Company. The authors would like to thank Dr. P. Geis and Dr. S. Donaldson of the Procter & Gamble Company for holding constructive discussions with us and for reviewing the manuscript. We also thank Mr. Tottori of Kogaku Inc. for his support for and input into the microscopic system designs. One of the authors, H. Matsuoka, acknowledges support from Grant-in-aid for Scientific Research for the Promotion of Safety and Security of Foods, The Ministry of Health, Labor, and Welfare.

REFERENCES

ASTM E2274-03 (2004) Standard test method for evaluation of laundry sanitizers and disinfectants.

Borkow, G., and Gabbay, J. (2004) Putting copper into action: copper-impregnated products with potent biocidal activities. *FASEB J.*, **18**, 1728-1730.

Buda, A., Sands, C., and Jepson, M.-A. (2005) Use of fluorescence imaging to investigate the structure and function of intestinal M cells. *Adv. Drug Deliv. Rev.*, **57**, 123-134.

Burton, K. (2003) An aperture-shifting light-microscopic method for rapidly quantifying positions of cells in 3D matrices. *Cytometry*, **A54**, 125-131.

Cen, L., Neoh, K.-G., and Kang, E.-T. (2004) Antibacterial activity of cloth functionalized with N-alkylated poly(4-vinylpyridine). *J. Biomed. Mater. Res.*, **A71**, 70-80.

Fujioka, K., Kozone, I., Saito, M., and Matsuoka, H. (2006) Rapid evaluation of the efficacy of microbial cell removal from fabrics. *J. Ind. Microbiol. Biotechnol.*, **33**, 995-1002.

Japan Industrial Standard L0844 (1997) Test methods for colour fastness to washing and laundering.

Japan Industrial Standard L1902 (2002) Testing for antibacterial activity and efficacy on textile products.

Petrocci, A. M., and Clarke, P. (1969) Proposed test method for antimicrobial laundry additives. *J. of AOAC*, **52**, 836-842.

Roldán, M., Thomas, F., Castel, S., Quesada, A., and Hernández-Mariné, M. (2004) Noninvasive pigment identification in single cells from living phototrophic biofilms by confocal imaging spectrofluorometry. *Appl. Environ. Microbiol.*, **70**, 3745-3750.

Staudt, C., Horn, H., Hempel, D.-C., Neu, T.-R. (2004) Volumetric measurements of bacterial cells and extracellular polymeric substance glycoconjugates in biofilms. *Biotechnol. Bioeng.*, **88**, 585-592.

Matsuoka, H., Oishi, K., Watanabe, M., Kozone, I., Saito, M., and Igimi, S. (2003) Viable cell detection by the combined use of fluorescent glucose and fluorescent glycine. *Biosci. Biotechnol. Biochem.*, **67**, 2459-2462.

McNally, J.-G., Karpova, T., Cooper, J., and Conchello, J.-A. (1999) Three-dimensional imaging by deconvolution microscopy. *Methods*, **19**, 373-385.

Yoshioka, K., Takahashi, H., Homma, T., Saito, M., Oh, K.-B., Nemoto, Y., and Matsuoka, H. (1996) A novel fluorescent derivative of glucose applicable to the assessment of glucose uptake activity of *Escherichia coli*. *Biochim. Biophys. Acta*, **1289**, 5-9.

A real-time method of imaging glucose uptake in single, living mammalian cells

Katsuya Yamada[1], Mikako Saito[2], Hideaki Matsuoka[2] & Nobuya Inagaki[3]

[1]Department of Physiology, Hirosaki University School of Medicine, Aomori 036-8562, and CREST of Japan Science and Technology Agency, Honcho 4-1-8, Kawaguchi, Saitama 332-0012, Japan. [2]Department of Biotechnology and Life Science, Tokyo University of Agriculture and Technology, 2-24-16 Nakamachi, Koganei, Tokyo 184-8588, and CREST, Japan. [3]Department of Physiology, Akita University School of Medicine, 1-1-1 Hondo, Akita 010-8543, and Department of Diabetes and Clinical Nutrition, Kyoto University Graduate School of Medicine, Kyoto, and CREST, Japan. Correspondence should be addressed to N.I. (inagaki@metab.kuhp.kyoto-u.ac.jp) about cell assays and to H.M. (mhide@cc.tuat.ac.jp) about 2NBDG synthesis.

Published online 29 March; corrected online 9 August 2007 (details online); doi:10.1038/nprot.2007.76

This protocol details a method for monitoring glucose uptake into single, living mammalian cells using a fluorescent D-glucose derivative, 2-[*N*-(7-nitrobenz-2-oxa-1,3-diazol-4-yl)amino]-2-deoxy-D-glucose (2-NBDG), as a tracer. The specifically designed chamber and superfusion system for evaluating 2-NBDG uptake into cells in real time can be combined with other fluorescent methods such as Ca^{2+} imaging and the subsequent immunofluorescent classification of cells exhibiting divergent 2-NBDG uptake. The whole protocol, including immunocytochemistry, can be completed within 2 d (except for cell culture). The procedure for 2-NBDG synthesis is also presented.

INTRODUCTION

Glucose is the major carbon source used in the cells of most organisms, so measurement of glucose uptake is an important research issue. In mammalian cells in particular, measuring glucose uptake of a heterogeneous population and/or differing activity status is of great interest[1,2]. To quantify glucose uptake, a variety of radiolabeled tracers such as [^{3}H] glucose[2], [^{14}C] 2-deoxy-D-glucose (2-DG)[3], [^{18}F] fluoro-2-deoxy-D-glucose[4] and [^{14}C] or [^{3}H] 3-O-methyl-D-glucose[5,6] have been used effectively. However, the spatial and temporal resolution of these methods is not high, and they cannot be used to visualize glucose uptake in single, living cells.

This protocol details a method for real-time monitoring of glucose uptake in single mammalian cells using a fluorescent D-glucose derivative, 2-[*N*-(7-nitrobenz-2-oxa-1,3-diazol-4-yl)amino]-2-deoxy-D-glucose (2-NBDG), as a tracer. 2-NBDG was initially developed for the rapid non-culture count of viable microbial cells and was successfully applied to *Escherichia coli*[7] and many other food-borne bacteria[8]. It has since been demonstrated in living mammalian cells that the uptake of 2-NBDG takes place through glucose transporters (GLUTs) in a concentration-, time- and temperature-dependent manner[9]. A short-period application of 2-NBDG produced a remarkable increase in the fluorescence intensity in COS-1 cells over-expressing GLUT2, whereas the increase was barely detectable in mock-transfected cells[9]. In mouse insulin-secreting clonal MIN6 cells[10], uptake was inhibited by cytochalasin B, a specific blocker for GLUTs, and by D-glucose in a dose-dependent manner[9]. Kinetic analysis using fluorometry further revealed that the time course of the uptake into MIN6 cells was almost linear up to 2 min, and apparent K_m values calculated from the Eadie–Hofstee transformation using the initial velocity of uptake at 1 min were similar to those reported for D-glucose and the non-metabolizable glucose analog, 3-O-methyl-D-glucose, found in pancreatic islets and cultured β-cells[9].

In recent years, 2-NBDG has been shown to be useful for monitoring glucose uptake into a variety of mammalian cells. These include pig vascular smooth muscle cells[11], rabbit enterocytes[12], rat cardiomyocytes[13], rat and mouse astrocytes and neurons in culture and *in vivo*[14–18], human and murine tumor cell lines[19,20] and adipocyte cell lines[21]. Inhibition of 2-NBDG uptake by D-glucose has been confirmed using vascular smooth muscle cells[11] and tumor cell lines[20], and inhibition by cytochalasin B in rat astrocytes[15].

Direct visualization of glucose uptake without using isotopes makes the 2-NBDG method quite attractive[13,21,22]. In addition, 2-NBDG has recently been used to investigate cell type–specific uptake of glucose and intercellular communication, such as that in the CNS[14–16,18]. Simple superfusion of 2-NBDG over cells using a flow-through system allows simultaneous monitoring of differing glucose uptake into heterogeneous cells. However, care should be taken because fluorescence intensity is an arbitrary measure. Thus, quantification requires stability of the system as well as accurate procedures. Accordingly, we focus here on the construction of a flow-through system as well as a practical protocol for measurement of 2-NBDG uptake. Also presented are procedures for combining this method with Ca^{2+} imaging by fura-2 and subsequent immunocytochemical identification of cells[9].

The limitation in the use of 2-NBDG is related to its intracellular fate. We previously found that 2-NBDG is metabolized to a phosphorylated fluorescent derivative at the C-6 position (2-NBDG 6-phosphate) after entering into *E. coli* cells and then decomposes to a non-fluorescent derivative[23]. Thus, the fluorescence intensity should reflect a dynamic equilibrium of generation and decomposition of 2-NBDG and the fluorescent metabolite. The use of 2-NBDG in the study of intracellular glucose metabolism is thus limited, and experiments must be carefully performed.

The protocols for 2-NBDG synthesis are described as well as the detailed characteristics of 2-NBDG, for researchers who may want to use a large amount of purified 2-NBDG.

MATERIALS

REAGENTS

- DMEM containing 4,500 mg l^{-1} D-glucose (DMEM-HG) (Life Technologies, cat. no. 12800-082)
- MIN6 cells (see REAGENT SETUP)
- Ca^{2+}, Mg^{2+}-free (CMF) PBS (see REAGENT SETUP)
- Trypsin–EDTA (Life Technologies, cat. no. 25200-023)
- 2-NBDG (see **Box 1** and **Fig. 1**)
- Krebs Ringer bicarbonate buffer (KRB) (see REAGENT SETUP)

BOX 1 | SYNTHESIS OF 2-[*N*-(7-NITROBENZ-2-OXA-1,3-DIAZOL-4-YL)AMINO]-2-DEOXY-D-GLUCOSE (2-NBDG)

REAGENTS

- D-glucosamine (Sigma)
- $NaHCO_3$ (Kokusan Chemical)
- 4-Chloro-7-nitrobenzofurazan (NBD-Cl; Wako)
- Sephadex A-50 (Amersham Pharmacia)
- Sephadex LH-20 (Amersham Pharmacia)
- D_2O (100 atom %D; Aldrich)
- Acetonitrile (chromato-grade for thin-layer chromatography (TLC); Kokusan Chemical)
- Triethanolamine (TEA; Kokusan Chemical)
- TLC plate silica gel 60 F_{254} (Merck Japan Limited)

EQUIPMENT

- Rotary evaporator (N-1000; EYELA)
- Freeze-dryer (FD-1; EYELA)
- DEAE (2-(diethylamino)ethyl-) Sephadex A-50 column and Sephadex LH-20 column (see REAGENT SETUP below)

REAGENT SETUP

DEAE Sephadex A-50 column and Sephadex LH-20 column Equilibrate DEAE Sephadex A-50 and Sephadex LH-20 with dH_2O, and fill into respective glass columns according to the standard protocols recommended by the company. The resin volume is 30× 200 mm^2 (diameter times length) for DEAE Sephadex A-50 and 20 × 250 mm^2 (diameter times length) for Sephadex LH-20. Operate both columns according to the standard protocol of gel filtration.

PROCEDURE

1. Dissolve 0.5 g D-glucosamine in 10 ml 0.3 M $NaHCO_3$ solution in a 100-ml Erlenmeyer flask (solution A), and dissolve 0.5 g NBD-Cl in 20 ml methanol in a 50-ml beaker (solution B).
2. Mix solutions A (10 ml) and B (20 ml) in a 100-ml recovery flask (egg plant flask). Send N_2 gas into the flask to purge the inside air and finally seal the flask with a silicon rubber cork with a balloon filled with N_2 gas. Wrap the flask with aluminum foil to shield from light. Shake the flask in a water bath shaker at 30 °C for 18 h.
3. Remove precipitates in the reaction mixture by filtration through a nylon mesh (10 μm) (or glass wool) using an aspirator. Collect the filtrate in another recovery flask.
4. Evaporate the reaction mixture to remove the solvent. A slight amount of solvent remaining does not matter.
5. Add 10 ml dH_2O to the flask to dissolve the product (solution C).
6. Load solution C on the Sephadex A-50 column after filtration through a filter paper. Elute the column with dH_2O and collect yellow and orange fractions together. It is advisable to collect small fractions and then combine them after TLC (Step 7).
7. Frequently analyze the elute by TLC around the beginning and the end of the elution of yellow and orange components. This is done by performing these steps: (i) Spot 100-μl aliquots on the silica gel plate and develop with a solvent composed of $CH_3CN:H_2O = 17:3$ (v/v). (ii) Detect fluorescent spots under a UV illuminator. (iii) Heat the plate to visualize sugar spots. (iv) Determine the retention factors (R_f) of fluorescent spots and sugar spots. A typical result is shown in **Figure 1a.** R_f of 2NBDG is 0.68.

Note: Maximize the 2NBDG yield but minimize the collection volume to be treated in the next step. Typically, the collection volume is approximately 200 ml (solution D).

8. Reduce the volume of solution D to about 5 ml by evaporation. Observe the solution volume carefully and stop evaporation before the volume becomes too small (this is solution E).
9. Load solution E on the Sephadex LH-20 column. Elute the column with dH_2O. Yellow, orange and brown fractions follow in that order. Collect the orange fractions.
10. Frequently analyze the eluate by HPLC around the beginning and the end of elution of the orange component. This is done by following these steps: (i) Inject 2–5-μl aliquots into the sample injection port and elute with solvent composed of $CH_3CN:H_2O = 17:3$ (v/v). (ii) Adjust the elution speed to 0.5 ml min^{-1} and monitor the optical density of the eluate at 475 nm. A typical result is shown in **Figure 1b**. The peaks at 10.5 min (P_1) and 11.8 min (P_2) represent the β-D-anomer and α-D-anomer of 2-[*N*-(7-nitrobenz-2-oxa-1,3-diazol-4-yl)amino]-2-deoxy-D-glucose (2-NBDG), respectively. (iii) Estimate the purity using the formula (P_1 area + P_2 area)/(All peaks) × 100%.

Note: This is done to find the optimal condition to collect a maximum amount of 2-NBDG with highest purity. Successful gel filtration gives more than 98% purity.

11. Collect fractions containing 2-NBDG of more than 98% purity (solution F). Expected volume is 5 ml per fraction × 15–20 fractions.

Note: In case of low purity, repeat gel filtration using a fresh Sephadex LH-20 column.

12. Reduce the volume of solution F to approximately 10 ml by evaporation (solution G).
13. Freeze solution G in liquid N_2 to lyophilize the product. A yield of approximately 100 mg is expected.

Note: Dissolve the dry matter with dH_2O and store at 4 °C and use within 4 weeks. Keep the dry matter at −20 °C for longer storage.

14. Confirm the identity of the product by proton nuclear magnetic resonance analysis (^{1}H-NMR). Dissolve the dry matter of the product with deuterium oxide and immediately analyze it using ^{1}H-NMR under 500 MHz. A typical result is shown in **Figure 1c**. Assign peaks to respective protons of pyranose and NBD.

BOX 1 | CONTINUED

15. Analyze the mass spectrum by fast atom bombardment mass spectrometry (FAB-MS) (*m/z*) using triethanolamine as the matrix. Confirm the peak at 343 that corresponds to 2-NBDG-H$^+$.

16. Analyze the fluorescent spectrum according to the following steps: (i) Dissolve 2-NBDG with distilled water to adjust the concentration to 10 μg ml^{-1}. (ii) Measure emission spectrum from 495 to 650 nm under excitation at 475 nm. (iii) Measure the fluorescence intensity at 550 nm by scanning the excitation wavelength from 300 to 520 nm. (iv) Typical spectra depicted in **Figure 1d** will be obtained.

- D-Glucose (Wako)
- Cytochalasin B (Sigma, cat. no. C6762)

EQUIPMENT

- 35-mm culture dish with an oval glass bottom (14 × 5 mm^2, 0.08–0.12-mm-thick glass) (Matsunami Glass Ind., Osaka, Japan, cat. no. D110500) (**Fig. 2**) (see EQUIPMENT SETUP)
- Cover glass (cut into 10 × 11 mm^2 pieces) (Corning, cat. no. 1)
- Vacuum grease (HVAC-G; Shin-Etsu Silicone, Tokyo, Japan)
- Round-type, heating glass stage with a flat surface (0.5 mm thick, MPF-10HF) (Kitazato Supply, Fuji, Shizuoka, Japan) or equivalent
- Superfusate warmer (MT-1, dead volume = 0.13 ml; Narishige, Tokyo; or SF-28, Warner)
- Thermistor probe (IT-23, diameter = 0.23 mm; World Precision Instruments)
- Digital thermometer (TH-5; Physitemp Instruments, Clifton, NJ)
- Inverted microscope (Nikon DIAPHOT TMD300 or equivalent) equipped with long working distance (WD) objective lenses: Nikon CF Plan ×2 (NA 0.05, WD 5.8 mm), Plan ×4 DL (NA 0.13, WD 16.2 mm), Plan ×10 DL (NA 0.3, WD 9.2 mm) and Plan Fluor ×20 DLL Ph2 (NA 0.5, WD 2.1 mm) or Plan ELWD ×20 DL Ph2 (NA 0.4, WD 7.0–8.1 mm)
- Dichroic mirror (DM), excitation (Ex) and barrier (BA) filters used for 2-NBDG measurement are Nikon DM 505, Ex 480/40 and BA520–560, respectively
- Neutral density (ND) filters: Nikon ND2 (50%), ND4 (25%) and ND8 (12.5%) for fluorescent imaging; ND2 and ND16 (6.25%) for transmitted light imaging; variable intensity is obtained by using these filters in combination
- Peristaltic pump (MCP Standard pump equipped with 12 roller-pumphead MS/CA4-12; Ismatec SA, Glattbrugg, Switzerland)
- Vacuum pump (DAP-15; Alvac, Kanagawa, Japan)
- Vacuum pressure gauge
- Imaging system (Argus 50; Hamamatsu Photonics, Hamamatsu, Japan) or equivalent
- Silicon intensified target (SIT) camera (Hamamatsu Photonics) or equivalent

REAGENT SETUP

CMF-PBS NaCl, 137 g l^{-1}; KCl, 4.0 g l^{-1}; $NaH_2PO_4 2H_2O$, 0.36 g l^{-1}; KH_2PO_4, 0.18 g l^{-1}; $NaHCO_3$, 12 g l^{-1}; glucose, 11 g l^{-1}; pH 7.30–7.35.

KRB NaCl, 129 mM; KCl, 4.7 mM; KH_2PO_4, 1.2 mM; $CaCl_2$, 1.0 mM; $MgSO_4$, 1.2 mM; $NaHCO_3$, 5.0 mM; HEPES, 10 mM; pH 7.35–7.40.

Preparation of MIN6 cells (i) Prepare a total of 92 ml DMEM-HG containing 13% FBS (FBS-DMEM-HG) in two 50-ml tubes by adding 6 ml FBS to 40 ml DMEM-HG for each tube. (ii) Prepare two 10-cm culture dishes and add 10 ml FBS-DMEM-HG into each dish. (iii) Prepare 15 ml CMF-PBS. (iv) Prepare 1 ml trypsin–EDTA. (v) Warm (i–iv) at 37 °C for the following steps. (vi) Exchange medium in a 10-cm dish culturing MIN6 cells with 10 ml CMF-PBS. (vii) Suck CMF-PBS with a vacuum pump and add 5 ml CMF-PBS and 1 ml 0.25% trypsin–EDTA. (viii) After waiting for 1–2 min, peel off the cells gently by sucking and blowing the medium through a 10-ml pipette. (ix) Suck the cell suspension (approximately 6 ml) and transfer into 30 ml FBS-DMEM-HG. (x) Centrifuge at 1,500 r.p.m. for 3 min (in a Kubota 5200, Kubota Co., Tokyo, Japan). (xi) Suck the supernatant and add 10 ml FBS-DMEM-HG. (xii) Triturate five times with a 10-ml pipette (let cells go back and forth gently within the pipette using a Pipette aid). (xiii) Centrifuge at 1,500 r.p.m. for 1 min (in a Kubota 5200, Kubota Co., Tokyo, Japan). (xiv) Add 3 ml FBS-DMEM-HG. (xv) Triturate 40 times with a 5-ml pipette, and count cells within 30 s. (xvi) Dilute cell suspension at 20 × 10^4 ml^{-1}. (xvii) For passage, transfer 0.5 ml cell suspension into each of the 10-cm dishes containing 10 ml FBS-DMEM-HG (ii). (xviii) For the experiment, triturate 20 times again and transfer cell suspension (145 μl) onto the glass part of a glass-bottom culture dish. Moisten the glass part of the dish with 100 μl FBS-DMEM-HG beforehand and suck medium just before plating. (xix) Observe cells after waiting for 5 min and readjust the dilution ratio so that most cells are seen separately. If too many cells are observed, blow off cells with yellow tip and dilute again. (xx) Leave the cells in a CO_2 incubator (5% CO_2, 37 °C) for 30 min until the cells adhere to the glass. (xxi) Add 2 ml FBS-DMEM-HG to fill the whole culture dish. (xxii) Perform measurement of 2-NBDG uptake before many clusters of MIN6 cells are formed. To assess the health of MIN6 cells during the course of the passages, check [Ca^{2+}] responsiveness to glucose stimulation similarly to the procedure described in **Box 2** (**Figs. 2** and **3**).

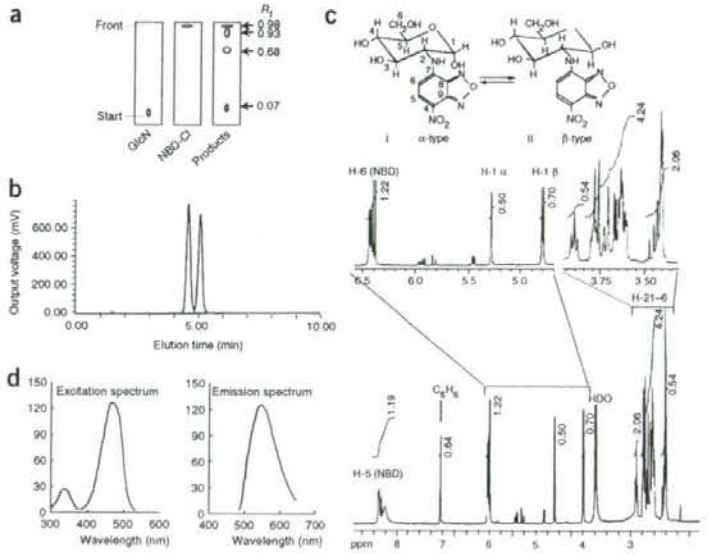

Figure 1 | Analytical data of 2-[*N*-(7-nitrobenz-2-oxa-1,3-diazol-4-yl)amino]-2-deoxy-D-glucose (2-NBDG). (**a**) TLC. Silica gel plate, solvent $CH_3CN:H_2O$ = 17:3, R_f (fluorescent spots: 2NBDG = 0.68, NBD-Cl = 0.98, GlcN = 0.07, unidentified by-products = 0.93). (**b**) HPLC spectrum. Column: TSKgel amide-80, eluent: $CH_3CN:H_2O$ = 17:3, flow rate: 1.0 ml min^{-1}, detection: $OD_{475\ nm}$. Two peaks: α-D-anomer and β-D-anomer. (**c**) ^{1}H-NMR spectrum. 500 MHz in D_2O, δ4.78 p.p.m. (d, $J_{1,2}$ = 10 c.p.s., axial–axial, β), δ5.27 p.p.m. (d, $J_{1,2}$ = 4 c.p.s., axial–equatorial, α), δ3.4–3.95 p.p.m. (m, H-2–H-6), δ6.4 p.p.m. (*m*, H-6 NBD), δ8.2–8.35 p.p.m. (*m*, H-5 NBD). (**d**) Fluorescence spectra. Emission spectrum: λ_{EM} = 495–650 nm, λ_{EX} = 475 nm; excitation spectrum: λ_{EM} = 550 nm, λ_{EX} = 300–520 nm.